CHALMERS

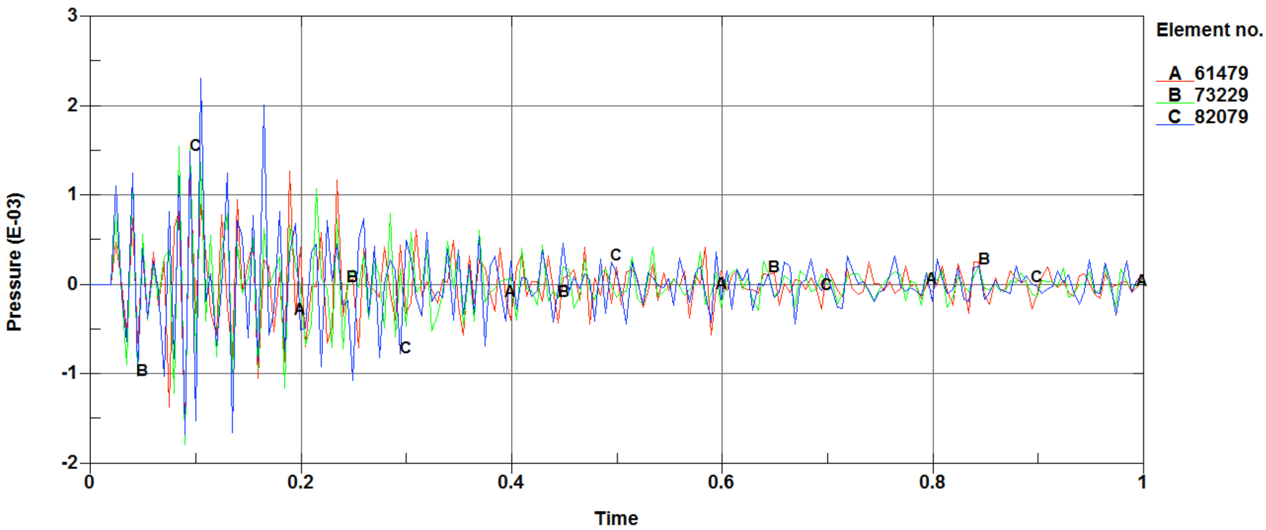

Simulation of Pressure Wave Propagation in the Brain

Master's thesis in Applied Mechanics

MARIE NYDAHL

Department of Applied Mechanics
Division of Vehicle Safety, Injury Prevention Group
CHALMERS UNIVERSITY OF TECHNOLOGY
Göteborg, Sweden 2014

Master's thesis 2014:59

MASTER'S THESIS IN APPLIED MECHANICS

Simulation of Pressure Wave Propagation in the Brain

MARIE NYDAHL

Department of Applied Mechanics
Division of Vehicle Safety, Injury Prevention Group
CHALMERS UNIVERSITY OF TECHNOLOGY

Göteborg, Sweden 2014

Simulation of Pressure Wave Propagation in the Brain
MARIE NYDAHL

Master's thesis 2014:59
ISSN 1652-8557
Department of Applied Mechanics
Division of Vehicle Safety, Injury Prevention Group
Chalmers University of Technology
SE-412 96 Göteborg
Sweden
Telephone: +46 (0)31-772 1000

Cover:
Pressure measurements in gel simulation LS-DYNA model

Chalmers Reproservice
Göteborg, Sweden 2014

Simulation of Pressure Wave Propagation in the Brain
Master's thesis in Applied Mechanics
MARIE NYDAHL
Department of Applied Mechanics
Division of Vehicle Safety, Injury Prevention Group
Chalmers University of Technology

Abstract

Stunning quality in the slaughter house varies. A growing concern for the animals well-being and the safety of slaughter house personal call for improved slaughtering techniques. The main aim of this thesis is to establish whether or not the external parameters of a bolt stun can be altered to improve the stunning quality of animals before a debleeding.To meet this aim three sub studies, using finite element models and the solver LS-DYNA, were carried out. First, experiments in which a bolt entered gel bodies were reproduced to suggest modeling strategy and contact settings. An ALE method for the modeling was determined to be the most appropriate. Second, a finite element model of a rat brain was adopted and evaluated. Past experiments, carried out on rats, in which pressures were recorded in the brain during simulated stunning, served as evaluation data. Some problem areas in fitting the FE model to this purpose were identified, mainly areas where pressure transfer was hindered. Finally, a parameter study was carried out to study the effect of external bolt parameters in intra cranial pressure distribution. The simulation results from the parameter study indicate that a change of speed, position and angle could greatly affect how the pressure propagates through the brain tissue, and thereby increase the quality of the animal stunning.

Keywords: Pressure propagation, LS-DYNA, ALE, FSI, MMALE, Penetration damage, Rat brain model

Acknowledgements

This thesis could not have been achieved without the support and guidance from my supervisor Johan Davidsson (Chalmers University of Technology).
I would also like to thank Karin Brolin (Chalmers University of Technology) and Ruth Paas (Chalmers University of Technology) for their help, and patience, with my material modeling and simulation questions.
A special thanks to Jacobo Antona (Japan Automobile Research Institute) who provided me with the rat brain model and was available to answer any of my questions.

Marie Nydahl
Göteborg, Sweden, 2014

Abbreviations and Nomenclature

ALE = **A**rbitrary **L**agrangian **E**ulerian Method
MMALE = **M**ulti-**m**aterial **A**rbitrary **L**agrangian **E**ulerian Method
FSI = **F**luid **S**olid **I**nteraction
FE = **F**inite **E**lement
CSF = **C**erebro**s**pinal **F**luid
RBM = **R**at **B**rain **M**odel

λ = wavelength, [m]

f = frequency, $\left[\frac{1}{s}\right]$

c = light velocity, $\left[\frac{m}{s}\right]$

G = relaxation shear modulus, [Pa]

G_0 = short time shear modulus, [Pa]

G_{inf} = long time shear modulus, [Pa]

ρ = density, $\left[\frac{kg}{m^3}\right]$

β = decay constant, [-]

τ_i = relaxation times, [s]

Contents

1 Introduction

The industrialization of meat production puts high demands on effectiveness and safety, while societal concern for animal welfare has risen. Among these areas of concern are the driving of animals to stun pens, and also the method by which the animals are stunned before bleeding and killing. This has included evaluations of stun quality and the implementation of stun quality audit programs. EU regulations on cattle stunning states that it should be rapid and effective. This to make sure that the animal remains unconscious until debleeding, which should be initiated as soon as possible after stunning. It is believed that the current method of stunning animals during meat production can be improved.

Stunning quality has been suggested to be a function of pressure wave propagation into the brain stem region of the animal brain. This thesis aims at improving the understanding of pressure propagation in the brain by the use of the finite element technique.

This chapter presents the existing method by which stunning is performed and relevant brain anatomy and functions. The following chapters presents the finite element method used, mathematical material modeling, the existing rat brain model and finally the experiments that have been conducted in the past and that could serve as model evaluation data.

1.1 The Brain

To understand the stunning mechanism the anatomy and functions of the brain are investigated. A brain consists of a number of components (see Figure 1.1), such as the thalamus, the cerebellum, the hypothalamus and the cerebrum. Among them is also the brainstem, which contain the midbrain, and is presented in further detail below.

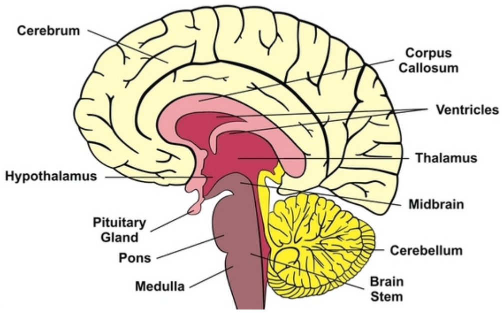

Figure 1.1: *Human brain, [1]*

The function of the brain is to exert centralized control over the other organs in the body. Some basic responsiveness such as reflexes can be mediated by the spinal cord or peripheral ganglia. As a rule, brain size increases with body size, but not in a simple linear proportion. Smaller animals tend to have larger brains, measured as a fraction of body size. Brain ventricles are the fluid filled areas of the brain, where measurements are most commonly taken. The ventricles are filled with a clear, colorless fluid called cerebrospinal fluid, CSF. The CSF cushions blows to the head and reduces the weight of the brain

1.1.1 Centers suggested to control consciousness

The nerve connections of the motor and sensory systems from the main part of the brain to the rest of the body pass through the brainstem, which is structurally continuous with the spinal cord, see Figure 1.2. It also has control of the heart rate and breathing. The midbrain controls basic functions such as sight, hearing and motor control. Together, the brainstem and the midbrain affect the central nervous system, the sleep cycle and consciousness. These are the areas targeted in stunning.

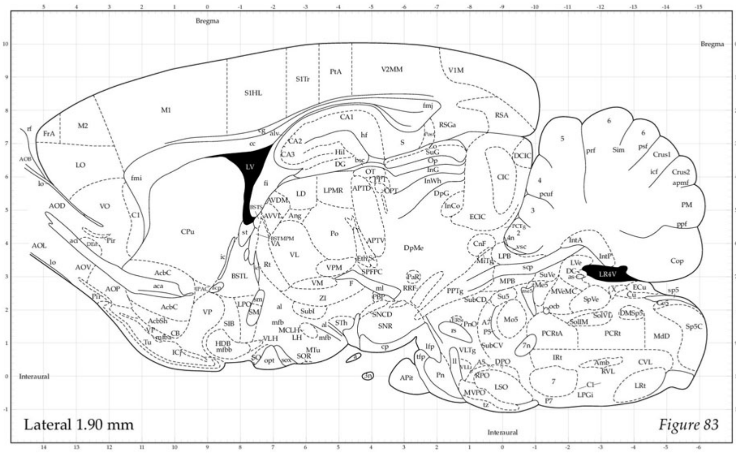

Figure 1.2: *Rat brain atlas*

1.2 Stunning

One of the most common ways of stunning is captive bolt stunning, whereby a metal bolt is propelled from a stun gun. This is initiated by a blank cartridge, or by air pressure in pneumatic stunners. The blank is placed in a chamber behind the bolt, which is then driven through the skull of the animal, creating a deep, penetrating brain injury. The cartridge charge controls the velocity of the bolt. There also exists non-penetrating methods for stunning.

When using the correct technique for stunning, including choice of stun gun, cartridge, pressure and angle, captive bolt stunning is expected to have a 100% success rate. If the stun is performed correctly the unconsciousness should last up to 10 minutes or longer. If a mis-stun should arise, the animal should be immediately re-stunned and bled. Signs of a poor stun quality include rolled eyes and rhythmic breathing. Rather than changing the existing equipment already in use, an alteration of how the equipment is currently used may be able to provide a more efficient stunning. In attempting to knock out the area around the brain stem, cattle is stunned by placing the stun gun against the forehead. An angle of 90 degrees between gun and skull is generally used. Changing the angle or position of the stun gun is believed to change the resulting pressures in the brain. If the path of the pressure in the brain can be established, this can be used to determine which external parameters to change in order to aim the pressure to the correct areas.

1.3 Pressure Propagation

The pressure wave that propagates through the brain during the stunning is initiated by the bolt hitting and penetrating the skull and brain. Pressure is a relationship between a force applied on a specific area. Therefor pressure in itself does not have a direction. This is problematic when searching for the shape of the pressure propagation.

Pressure moves in waves, with areas of high pressure and low pressure moving through an area. A pressure wave typically reaches a peak overpressure wave, followed by a negative pressure wave. In a blast or sudden impact situation, a peak positive pressure is expected to be followed by a large negative pressure, and finally an "evening out" of the pressure. Since waves reflect from various boundaries, the analysis of the time-profile of a pressure wave is very complex [2]. Previous studies have generally dealt with pressure in a brain over a long period of time, often with the goal of establishing the existence of permanent brain damage caused by blasts or explosions.

1.4 Studies using animal, analytical and FE-models to understand stunning performance

Previous studies on brain injury or trauma are generally focused on rotational trauma, blast effects and closed cranium pressure. Great efforts have been put into establishing working models of the brain and skull for different species.
Krave [3] studied the modeling of diffuse brain injury by creating, and investigating, a rabbit brain and skull FE-model. Wittek and Omori [4] researched the simulation of brain-skull boundary conditions for a human head, with a simplified brain-skull model. Kleiven and von Holst [5] examined the consequences of head size in relation to trauma, with a human head FE-model.
Pearce et al. [6] investigated pressure response in the human brain during short duration impacts, using three different FE-models of the human head, with varying biofidelity. Deck and Willinger [7] reported on the state of human head FE-modeling and stated that no model has been particularly exact when modeling pressure. Liu et al. [2] found that the reflections of the different boundaries complicated the analysis of the pressure. Brands [8] investigated mechanical responses in the brain during a closed head impact, finding them dominated by different wave propagations. Chafi et al. [9] assessed the brain dynamic responses due to blast pressure waves, using an FEM formulation of the human head, with a fluid-structure interaction algorithm.
Zhang et al. [10] examined the caviation and pressures in a brain simulant gel, creating a penetrating damage similar to the damage from a stunning bolt. Zhu et al. [11] used a gel surrogate to establish the biomechanical response during a shock wave, where they found that changing the orientation of their model greatly affected the pressures.

1.5 Aim

The aim of this thesis is to study how the stun quality is affected by the techniques used. In the thesis finite element models are used to study how pressure propagation in an animal brain model can be altered when stunning bolt characteristics are modified.
First, an experiment with gel bodies was reproduced to suggest the ideal simulation method to study pressure wave propagation through a uniform media that resembles brain tissue. Second, a pre-existing state of the art LS-DYNA Finite Element (FE) model of a rat brain and skull was adopted and evaluated. Data from experiments on anesthetized rats carried out in the past (Davidsson et al 2014) served as evaluation data. Third, this rat model was used for principle investigation of pressure propagation in the brain as a function of external stunning parameters.
The thesis was carried out at the Division of Injury Prevention, at the Department of Applied Mechanics at Chalmers University of Technology, in collaboration with Swedish University of Agricultural Sciences in Skara and Neurosciense at Karolinska Institute in Stockholm.

2 Background

In this chapter the Finite Element method and some relevant terms are introduced. The existing FE-model of the rat brain and skull are presented, as well as the past experiments on gel samples and rats, that produced the verification data.

2.1 The Finite Element method

The finite element, FE, method is a mathematical approximation that solves partial differential equations, by creating a mesh, connected by nodes for which the material behavior is prescribed. The FE method is generally implemented on computer models that are subjected to loads, and then analyzed to determine if certain criteria are met. It is used in cases when physical testing is expensive or impossible. The software LS-DYNA is primarily an explicit FE code, which means it has a less demanding time step calculation than the implicit time integration. This is advantageous in short physical time analysis such as impact simulation. By prescribing a material, boundary conditions, and material behavior equations to the model, different load cases can be solved. LS-DYNA works by reading specific control cards for each function implemented in the model. For solving complex problems the FE method is very powerful. When dealing with deformation a classic Lagrangian method is the most common approach. When dealing with large deformations however, the

Lagrangian method loses some of its accuracy. The Arbitrary Lagrange-Euler, ALE, approach is sometimes used to resolve large mesh distortions, where the Lagrangian method would be to costly.

2.1.1 Material Modeling

The brain tissue material model validation was based on parameters used in previous studies.
Bradshaw and Morfey [12] established that pressure is dependent mainly on the density of the material. Shear or bulk modulus was found to not affect the pressure to any large extent. The brain tissue material has previously been modeled in a variety of ways. According to Kleiven and von Holst [5] the central nervous system tissue is often modeled as having non-linear behavior. According to Brands [8], the non-linear, time dependent material behavior is also nearly incompressible, since the bulk modulus is around 10^6 times larger than the shear modulus. Biological tissue is often modeled as being a viscoelastic solid. Wittek and Omori [4], Krave [3], Antona et al. [13] and Deck and Willinger [14] model it with viscoelastic properties, while Chafi et al. [9] uses hyper-viscoelastic modeling.

Even in experiments and reports that dealt with the same species, very different material parameters have been implemented. Antona et al. [13] that created the rat brain model that was used, modeled it as a general viscoelastic material, with different Prony parameters, (eq. 2.1), for different regions of the brain. This was problematic when trying to verify the accurateness of each areas material parameters, see Figure 2.1. Antona et al. [13] used physical tests as a basis for the material parameters, but also stated that the material model might be an error source. Calculation of the relaxation shear modulus with Prony parameters:

$$G(t) = G_{inf} + \sum_{i=1}^{N} G_i e^{-t/\tau_i} \tag{2.1}$$

	G∞[Pa]	G1	τ1	G2	τ2	G3	τ3
Brainstem & Spine	240	1387	0.012	353	0.160	217	2.75
Cerebellum Grey	189	1391	0.009	353	0.226	240	5.37
Cerebellum White	169	1308	0.011	347	0.193	197	4.13
Corpus Callosum	208	1249	0.015	381	0.239	230	4.52
Hippocampus	528	1897	0.017	636	0.244	439	4.72
Cortex	433	1113	0.019	393	0.314	261	4.92
Thalamus & Bulbus olfactorius	347	1533	0.017	464	0.318	312	6.66

Figure 2.1: *Prony material parameters for RBM according to [13]*

The Boltzmann parameters, (eq. 2.2), found in Table 2.1, were taken from Krave [3]. These experimental parameters were taken from rabbits, so they may not be completely corresponding to the correct material properties for the Sprauge-Dawley rats.
Calculation of the relaxation shear modulus with Boltzmann parameters:

$$G(t) = G_{inf} + (G_0 - G_{inf})e^{-\beta t} \tag{2.2}$$

2.1.2 ALE & FSI

Modeling large deformations is often more accurately achieved using the ALE method. When defining a section of the model, the type of elements used for calculation need to be defined. When using a pure Lagrangian element type, the nodes of the mesh are seen as attached to the material. As the material moves and deforms, the nodes of the mesh do the same. The elements therefor contain the same material throughout the calculation. Because of this, large deformations of the material can create inaccuracies at large element distortion.
Eulerian elements are defined such that they are fixed in space, with material flowing through them. This is done by firstly deforming the material, as in the Lagrangian method, and then advecting, or remapping, the elements back to their original position in the mesh.

Table 2.1: Boltzmann parameters according to [3]

Parameter	Value
ρ	1040
K	$2.19\ 10^9$
G_0	1.72110^3
G_{inf}	5.0810^2
β	0.125

When Chafi et al [9] simulated blast pressure wave propagation in air and in the head the Arbitrary Lagrangian-Eulerian (ALE) multi-material method was used. With the ALE method two meshes are created. One is a background mesh that can move in space, and the other is a mesh attached to the material which flows through the moving mesh. It is initially deformed as the Eulerian mesh, but the advecting is instead performed onto the moving background mesh.
A void mesh may be necessary when implementing ALE. This is to make sure that the material has an area to deform into. Otherwise the material may simply stay inside its initially defined mesh. If the material has a large movement, the void can be set to move and deform with the material. The void has to be connected to each of the nodes on the surface of the material to be able to allow deformation of the material.This also meant that their nodes had to be merged. Voids can intersect other materials, but need to be merged with any intersecting void to make sure that the material can move correctly through the void.
There are different ALE elements available. Elform 11 is the most common, 1-point ALE multi-material element, which is very versatile. Elform 12 is a single material and void definition, limiting its use. When using Elform 11 the void material may be assigned as Mat_Vacuum, while with Elform 12 the void parts are simply prescribed as areas with 0 % of the material.

In LS-DYNA a part ID refers to a group of elements belonging to the same part, while an ALE-Multi-Material-Group ID refers to a region containing one physical material. This was used if there were multiple Eulerian materials being calculated. All the parts in the same group have identical material properties.
In Control_ALE the number of advection cycles, NADV, and mesh smoothing parameters can be defined. The number of advection cycles was set to one primarily.

2.1.3 Meshing

Hexahedrons are the most common mesh types used in LS-DYNA. However, if not looking at strains, a tetrahedral mesh might have given enough accuracy to work. The mesh had to be fine to give an accurate description of the pressure, so a large number of elements were required even from the start to give any sort of accurate indication of the models potential use.
For similar cases, although in different software, the recommendation is to use 5 elements per wave length. As seen in Eq. 2.3, an increase in frequency increases the necessary number of elements. According to Brands, [8], 24 elements per wavelength is necessary.

$$\lambda = \frac{c}{f} \tag{2.3}$$

Earlier research by Zhu et al, [11], shows that a 33% decrease in mesh size only had a 3% affect on the peak overpressure, while showing a more accurate shock front.
The LS-DYNA environment requires each element to be defined by a section, controlling the element behavior. Parts defined by Section_Solid are constant stress 8 node brick elements. When using ALE, Section_Solid_ALE was used.
When using a void mesh around the ALE material, the nodes on the boundary between them should had to be merged. The Lagrangian body, however, can overlap the ALE meshes.

2.1.4 Contact & Constraint

When a Lagrangian material hit another Lagrangian material, a Contact-function was necessary. In a one-way contact only the slave section is checked against penetration of the master section. The finer of the meshes should be defined as the slave section. In two-way contacts, the penetration detection is symmetrically performed. The coupling is performed via nodal contacts, and is either penalty based or constraint based. Penalty based coupling checks for penetration of the Eulerian and Lagrangian surfaces. This requires a stiffness parameter, that is primarily found through trial and error, as well as by a controlled, very small time step for stability. Other factors, such as damping and penalty factor, can also be controlled.

When a Lagrangian material hit an ALE material, a control sequence for a constrained Lagrangian in solid had to be added. In Cnstrnd_Lagrange_in_Solid the ALE was denoted as the master section, and the Lagrangian was set as the slave section. The Lagrangian mesh may intersect the ALE mesh, but the nodes were not shared between ALE and Lagrangian parts.

2.2 Existing FE-model

An FE model of a rat head, brain and neck has been created by Jacobo, et al., [13], into which the pressure analysis method was to be implemented. The purpose of the original model was to examine rotational trauma. The model was created by using Computed Tomography (CT) scans and Magnetic Resonance Images (MRI) of Sprague-Dawley rats to generate a geometry of the skull. An FE mesh based on the brain Atlas and the MRIs were combined to obtain a correct definition of each brain region. The final model differentiates between the skull, olfactory bulb, thalamus, brain stem, cerebrum, corpus callosum, hippocampus, cerebellum and neck. The model was also scaled down by a ratio of 1.11, to fit the average rat size used in experiments. Through further analysis different material properties could be established for the different brain regions, and the model was also experimentally verified for rotational trauma. The model consists of 147036 elements, with the skull mesh consisting of 33490 quad elements of approximately 0.4 mm size. The brain is meshed with 79469 hexahedral elements with an approximate average size of 0.35 mm. The material parameters for the general viscoelastic materials used can be found in Appendix B. The brain kinematics was validated by a comparison with experiments, where a thin pin was used to scar the brain cortex during a rotational trauma.

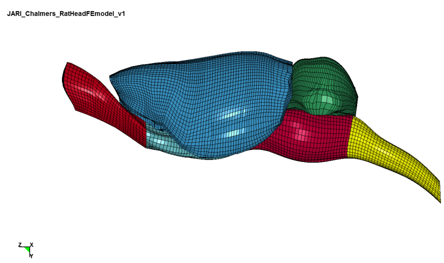

Figure 2.2: *Existing FE-model of the brain, without skull and neck*

2.3 Past penetrating stunning experiments carried out on gel samples

The main point of the simulated gel model was to be able to test and vary the material and contact parameters to find a realistic simulation method.

The initial gel experimental model is setup in the shape of a cylinder cut in half. Sensors are inserted at 0°, 30° and 60° angle from the impact point of the bolt, as can be seen in Figure 2.3. The material for these tests was a gel, created to mimic the brain tissue behavior.

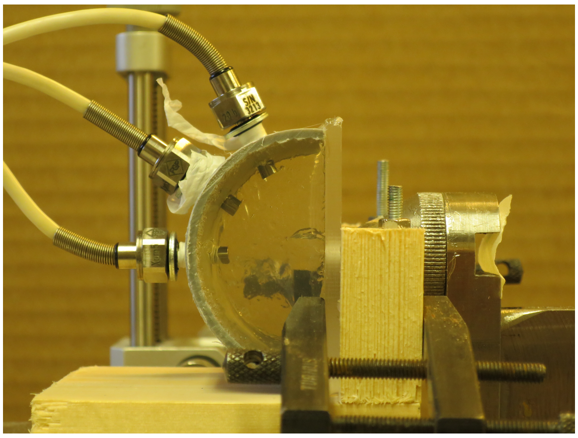

Figure 2.3: *Experimental gel test setup*

The gel was contained in a semi-rigid shell that was open at the sides. For the bolt to be able to penetrate the gel, a hole was placed at the top of the shell. The bolt creates a penetrative damage, that was about 5 mm deep, in accordance with the physical experiments.

2.4 Past penetrating stunning experiments carried out on rats

Physical experiments were carried out, by Johan Davidsson, to measure pressure variation in the brain during conditions that imitate bolt stunning. Following the deep anesthetization of Sprauge-Dowley rats a mid-line incision was made through the skin and periosteum. A burr-hole was drilled at 2 mm posterior, and 2 mm lateral to bregma. An aluminum impactor probe was positioned to enter the burr-hole, with the rat placed in a stereo-tactic frame. The path of the impactor probe was controlled by a narrow tube. Using a modified air rifle, a lead pellet was shot at the probe which then entered the dura at a speed of approximately 100 m/s. The air rifle pressure level was adjustable. The penetration depth was limited by the setup, to be varied between 2 to 6 mm. The impactor probes were flat tipped or rounded. By scaling of a stun gun used for bovine stunning, a diameter of 2 mm was chosen for the probes. Samba Sensors were used to record the pressure during the penetration. The experiments were approved by the local ethics committee.

3 Method

The objective of the thesis was to identify if an adjustment of external parameters affect the pressure propagation through the brain, and thereby the stun quality. Most of the research in the area of intracranial pressure has been performed by the automotive industry, or by military researchers. As a consequence of this most of the previous studies dealt with human heads during acceleration or external non-contact blasts.

Some literature (Chafi [9]), claimed that human brain tissue is approximately 30% stiffer than bovine or porcine brain tissue, which would indicate that the parameters are not directly transferable. An increase in head size is said to increase the maximum effective stress as well as the magnitude of the pressure, according to Kleiven [5].

The FE-software LS-DYNA R7.1.1 was used as the main analysis tool.

3.1 Reconstruction of the gel model to guide FE modeling strategy

The initial simulation was performed on a simple geometrical shape, which represented the brain tissue. The tissue sample was then struck with a bolt, made from a rigid material, set to have the properties of aluminum. The resulting pressures were compared to the setup of experiments performed by Johan Davidsson, using a gel to simulate brain tissue behavior.

3.1.1 The mathematical model

The tissue was modeled as a solid. The materials that were tested were viscoelastic, hyperelastic, and general viscoelastic, defined by Prony series parameters. For the initial testing the parameters for brain cortex tissue was used. The elements tested were defined as Lagrangian and ALE.
A void mesh was created around the simulated brain tissue, to ensure that the tissue could deform, see Figure 3.1. Otherwise, when using the ALE method, the material would stay inside the initial area. Since we have a penetrating brain damage, the material should be able to move, deform, and expand.

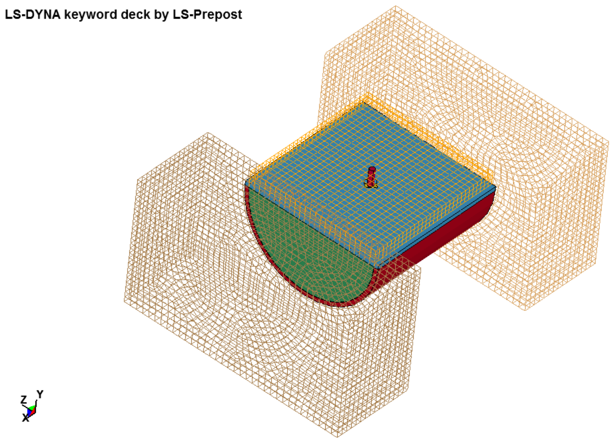

Figure 3.1: *Initial gel test model - Container, gel, bolt and surrounding void mesh*

The initial mesh was created using a mesh that conforms to the material, with the mesh lines following the outer contour of each Eulerian part. If using a simple orthogonal mesh where the mesh lines do not follow the contour, the volume fraction of the elements with mixed material had to be prescribed (Initial_Volume_Fraction).
The dimensional definitions used to establish the gel model are found in Table 3.1. Depth is defined as being in the z-direction, in accordance with Figure 3.1. D stands for diameter, while N represents the number of elements.

3.1.2 Modelling the loading conditions and constraints

The load was applied directly on the tissue as well as via a bolt created by rigid material. The bolt was given a prescribed velocity and a prescribed motion to get the penetration required. This meant that an FSI was needed to get the connection between the Lagrangian elements of the rigid material, and the ALE elements of the brain tissue model. The ALE elements were modeled with Elform 12 since the only ALE materials involved were the gel and the voids.
To control the contact between the bolt and the gel in the Lagrangian model, an automatic one way surface to surface contact was implemented. For the ALE a constrained Lagrange in solid control function was used. The control card for the constraint can create significant changes to the results. The appropriate type of coupling for these types of cases seemed to be a penalty coupling or a coupling that constrains acceleration and velocity. A direction of constraint had to be determined. It can be chosen to be applied in compression and tension, in only compression or in all directions. A number of coupling points also had to be chosen, which adds a spring force between the elements. An increase in the number of coupling points therefor would make for a stiffer coupling between the ALE and the Lagrange part. When the Lagrange mesh is coarser than the ALE mesh, the number of coupling points had to be increased above the default value, to avoid interspersing of the materials. A frictional constant may be defined, but due to a lack of appropriate data, and the high speed of the penetration, the frictional resistance was ignored.

3.1.3 Model evaluation

The model was verified by comparison with the results from the physical testing performed by Johan Davidsson. The material parameters was varied to establish whether or not a sufficiently correct model was used. The variations were performed according to Table 4.1. The initial values was chosen based on previous experiments.

Table 3.1: Model definitions

Part	No. of Elements	Dimensions
Half cylinder	160	D_{in} = 47 mm
		D_{out} = 50 mm
		Width= 50 mm
Plate	168	Depth= 50 mm
		Height= 1.5 mm
		Width= 50 mm
Bolt	36	Height= 6 mm
		D= 2 mm
		$N_y = 3$
		$N_d = 9$
Gel	402700	$N_x = 100$
		$N_z = 100$
		$N_{y,max} = 46$
Right/Left void	32340	Depth= 60 mm
		Height= 35 mm
		Width= 5 mm
Top void	560	Height= 4 mm
		Depth= 4.7 mm
		Width= 4 mm

The casing around the gel was constrained from any movement or rotation, and modeled as a rigid part. The motion of the bolt was prescribed as 100 m/s until it reaches a depth of 5 mm in the gel, after which the movement was stopped. The ALE meshes of the voids and the gel are locked in rotation and translation, since the material was not moving or deforming beyond the limits of the voids.

To further evaluate the method used, a comparison between the experimental pressures and the simulated pressures was performed. The experimental sensor were placed at a 0°, 30° and 60° angle from the entry point of the bolt, at a point inside the gel. The corresponding elements in the simulation were identified, as in Figure 3.2.

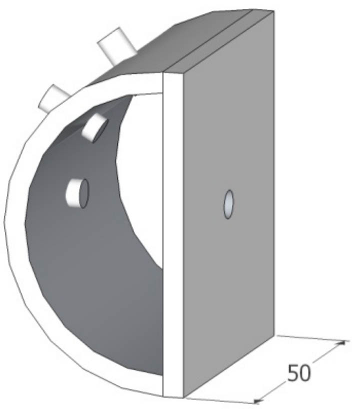

(a) *Gel mold experiment setup with sensors and bolt entry hole*

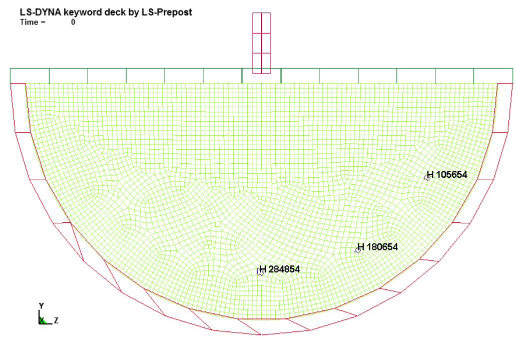

(b) *Data elements chosen at measuring points for the physical tests*

Figure 3.2: *Comparison between experimental setup and the reconstruction using finite element simulations*

More detailed specifications on material parameters, load curve definitions and contacts can be found in Appendix C.

3.2 Evaluation of the Finite Element Brain Model

The pre-existing rat brain model, (see Figure 3.4), was used to implement the methodology found in the theory, and by the simulations on the simplified gel model. The pre-existing meshing of the brain tissue was not altered. The original material parameters were kept, defining the brain as non-homogeneous.

3.2.1 The mathematical model

Since the brain tissue was chosen as non-homogeneous, a multi-material ALE, MMALE, method had to be used, and the voids were created as separate meshes. Each void mesh was surrounding one specific brain region, but belonging to the same MMALE group. This enabled their connection and overlap. The material specifications were not altered from the original model, but the element formulation for the brain tissue was set to be Elform 11.

The voids were created surrounding separate parts of the brain, with each void connected to one tissue-material as well as connected to the other voids, (see Figure 3.3). This was necessary to enable the transferal of material and forces through the gaps between the brain regions. Since the RBM is somewhat simplified, the gaps between the brain regions are larger than they would be in a physical brain.

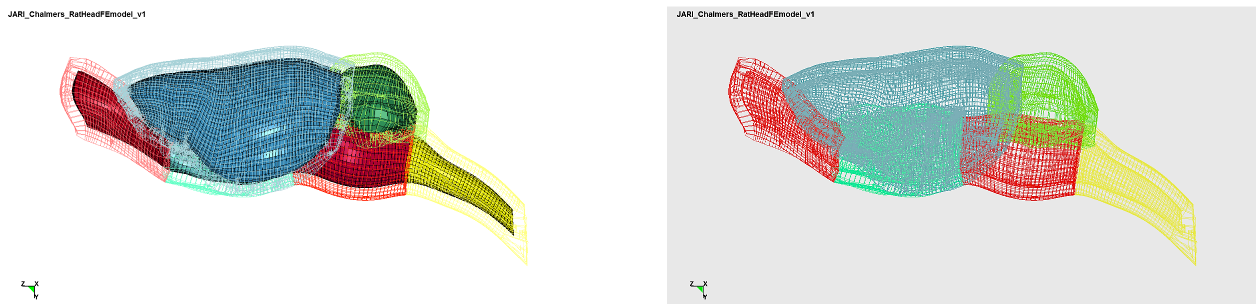

(a) *Voids attached to brain* (b) *Voids with brain hidden*

Figure 3.3: *Void meshes created, surrounding the brain regions*

The modeling of the voids was done directly as an offset from the surface in LS-PrePost. The offsets were set to be approximately 1 mm, with 4 elements of approximately 0.25 mm. The voids then had to be modified by removing the intersecting elements, that were automatically created. Some largely deformed void elements also had to be removed. After removal of the deformed or intersecting elements, the final 6 voids consisted of 64301 elements. Since the MMALE method does not work by simply defining the voids as empty of material, they are defined as vacuums, with a density of 0.001 kg/m^3.

3.2.2 Modelling the loading conditions and constraints

None of the reports that were found dealt with skull fracturing, only closed head impact. Since the skulls in the experiments had a direct contact between the bolt and the brain tissue, closed head impact pressure results were not directly transferable. The experiments used for validation were also performed with a pre-drilled hole through the cranium.

The boundary conditions on the brain are difficult to get right, and are commonly modeled as a sliding contact with the cranium, as done by Jacobo [13] and Kleiven [5]. Others, like Wittek [4] and Chafi [9] model the CSF as an 8-node solid with fluid-like properties, which is believed to generate the most accurate results [4]. The difference in densities between the skull and the brain, as well as the CSF surrounding the brain, mean that the brain is able to move relative to the skull. At the neck the boundary is sometimes modeled as free, as by Deck [14] and Chafi [9], or as constrained in selected points, as by Patel [15]. Since the experimental impact was fast and non-rotational, a sliding contact may have been put in; although Deck [14] hypothesized that if the time duration of the impact is short the neck will not influence the kinematic head response. Therefor the neck was ignored.

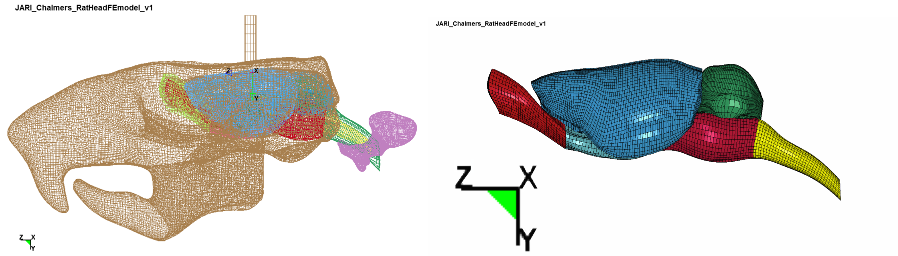

(a) *RBM with skull, neck bones and bolt*   (b) *RBM with coordinate system*

Figure 3.4: *Unaltered RBM*

The skull was completely constrained in space, while the contact between the skull and the bolt was chosen as non-existent. This eliminated the need to create a burr-hole in the skull through which the bolt could enter the brain tissue.

3.2.3 Model evaluation

The probes in the experiments were positioned according to Figure 3.5. Two standard positions for the probe can be found, one centered and one off-center. The size limitation of the brain meant that generally only one sensor at a time was used.

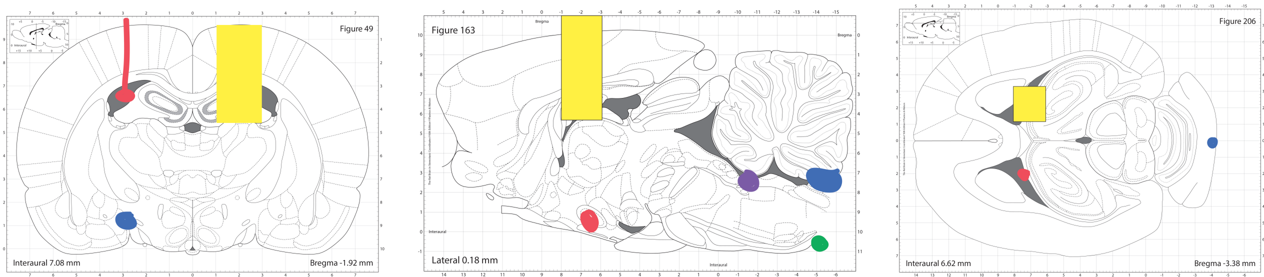

Figure 3.5: *Position of sensors and bolt (yellow) in different experimental setups*

The probe was modeled with 1320 rigid elements, 7 elements radially, 24 elements in the circumference and 10 elements high. It was locked in all directions and rotations, except the y-direction (see figure 3.4b), where it was given a speed of 100 m/s. The material of the probe was set to be a rigid material with the properties of aluminum. The skull was locked in all directions and rotations. More specifications regarding the variables set for each contact, curve, material et.c. can be found in Appendix C.
The simulation measurements were taken in the corresponding positions according to Figure 3.6. It is clear that the RBM does not have a complete correspondence with the rat brain atlas in Figure 3.5. The location of the sensors in the experiments are therefore approximated in the RBM, and a minimum of two elements are chosen to represent each sensor. The pressure measurements were filtered with a Butterworth 10 kHz filter.

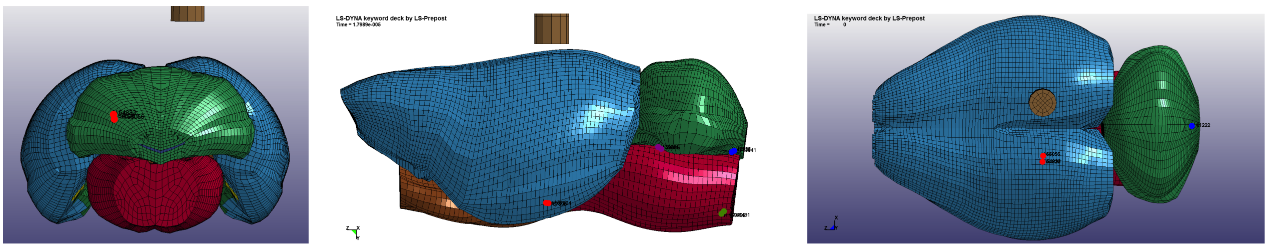

Figure 3.6: *Position of measuring elements and bolt in different simulations*

3.3 External Parameter Variations to study pressure propagation in the brain

To investigate how the external, changeable parameters may affect the pressure the position and the angle of the probe was changed. The probe was angled -10° and -20° around the x-axis. Elements around the final position of the probe were chosen for pressure output measurements, see figure 3.7. The probe curve and boundary conditions had to be modified from the previous testing, where its movements were restricted in all directions except in the y-direction.

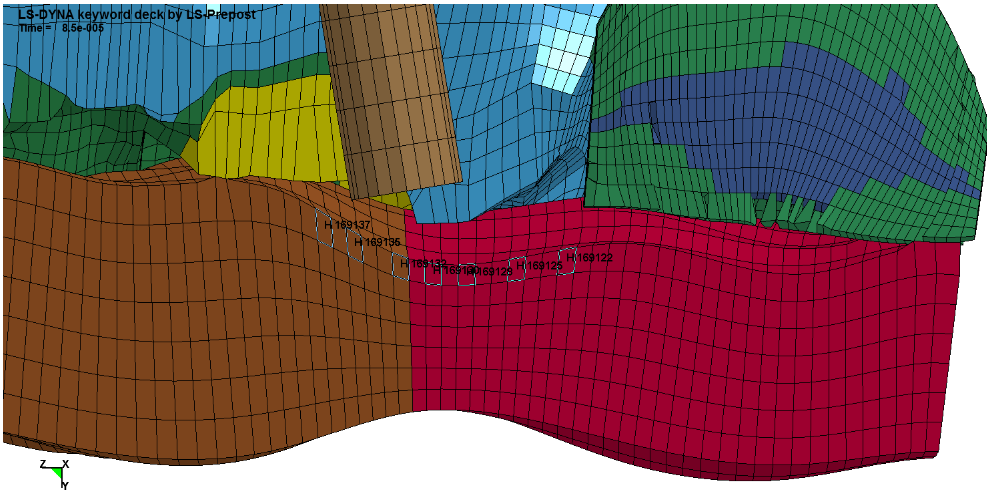

Figure 3.7: *Position of measurement elements after probe movement stopped, at 10°.*

The probe was also moved +2 mm and -2 mm, from the original position, along the z-axis. The measurement elements were chosen along the lower part of the brain, in an almost straight line along the z-axis, see figure 3.8.

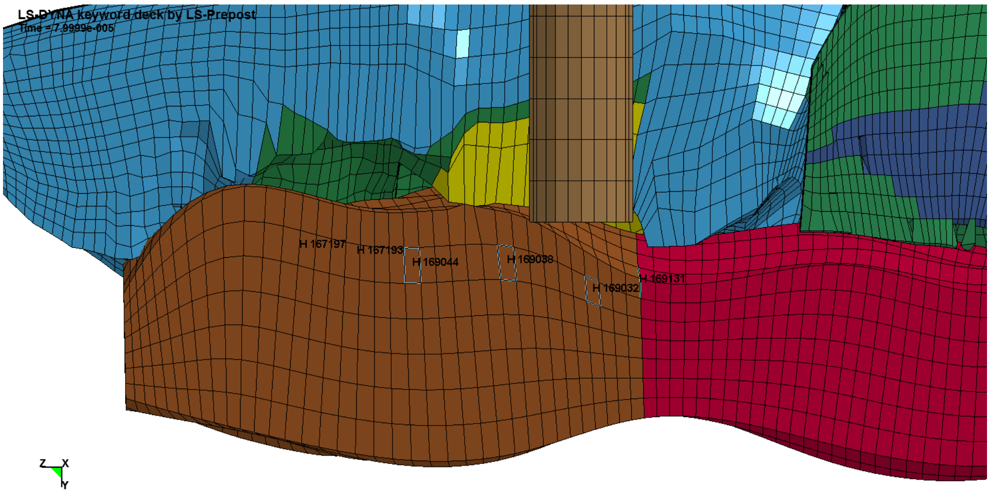

Figure 3.8: *Position of measurement elements after bolt is moved -2 mm.*

4 Results

The results of the primary search for a functioning material model, and the secondary application into the RBM are presented.

4.1 Gel Modeling

The initial purpose of the gel model was to determine if a Lagrangian method would be accurate enough, or whether an ALE method had to be implemented.
With the large deformations created, the ALE method was determined to be the most accurate for simulation. The Lagrangian method would have required a considerable refinement of the mesh. This would be possible in the gel model, but extremely time consuming in the final RBM. A correct pressure evaluation requires a very fine mesh, even in simple cases. The mesh would then have to be localy refined around the impact area of the bolt, but also along its entire path through the material. From the bolt path the refinement would also have to radiate outwards, to the edges of the material. With a very large and time consuming local refinement of the mesh, a pure Lagrangian model should be able to give accurate results as well.
It was determined that the most realistic way of transferring the force onto the gel would be to model the bolt as having a fixed velocity for a certain amount of time, until reaching the required depth. A velocity curve was therefor created, see Figure 4.1. The bolt was restrained from any other movement. The bolt was modeled as a rigid solid part, with the standard element form, Elform 1.

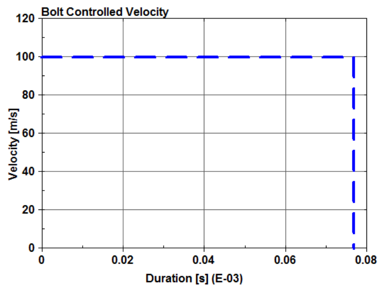

Figure 4.1: *Velocity curve of the bolt, [ms] vs [mm/ms]*

When testing the gel model a behavior corresponding to the experiments was found, according to Figure 4.2. The gel was pushed away from the bolt, creating a cavitation very similar to the physical experiments. The experiments by Zhang [10] found that the size of the cavities were generally 5-6 times that of the projectile diameters. Here however, the gel does not collapse back onto itself, forming a bubble as in the experiments. The probable cause of this was the fact that no air was simulated around the test setup. It was modeled as being in a vacuum. A possible cause may also have been that the gel was modeled after a brain material model, and not after the specific gel used. The gel material does not have a standardized material description, since it varies with the gel preparation method.

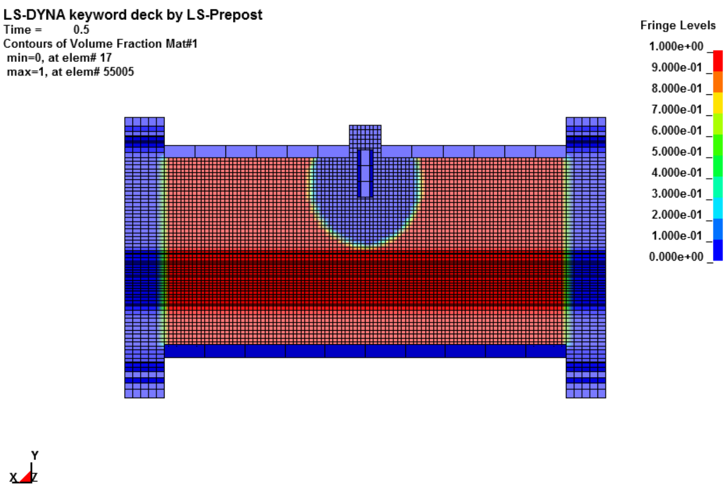

Figure 4.2: *Volume fraction of gel after bolt impact*

The elements between the gel and the void show up as blurred. This is because they share nodes that are half in the void and half in the gel.

By varying the material properties, the boundary conditions, and the contact between the bolt and the gel, the gel model was evaluated, see Table 4.1. The seemingly arbitrary changes to the shear relaxation was taken from different literature, using different material models. It became clear, as was also stated in some literature, that the main factors for the pressure distribution was the density of the material tested. Therefor the material chosen was simplified to a viscoelastic material, with parameters according to Krave [3].

Table 4.1: Variable Parameters

Parameter	Adjustment	Result
Time step DT	- 50 %	Large change in measured pressure output
Density	+ 10 %	Small change in pressure range
	+ 50 %	Increased pressure range, decreased pressure fluctuations
	- 20 %	Small change in pressure range, increased pressure fluctuations
Advection Method	Van Leer	No pressure change
	Energy Conservation	No pressure change
Pressure Iteration	Activated	No pressure change
ALE BC:s	BCTran=0; BCExp=7	Small change in peak pressure
	BCTran=0; BCExp=0	Small change in peak pressure
	BCTran=7; BCExp=0	Small change in peak pressure
Shear Relaxation	- 40 %	No pressure change, parameters according to [4]
	+ 2750 %	No pressure change , parameters according to [14]
	+ 30700 %	No pressure change, parameters according to [6]
ILEAK	Method 1	No pressure or deformation change
	Method 2	No pressure or deformation change

An increased fineness of the mesh and the timesteps also affected the resulting pressures that were found.

The gel simulations resulted in pressure measurements according to Figure 4.3, where blue, green and red measurements represent 0°, 30°and 60° offset, respectively. Further test data and pressure measurements are available in Appendix A.

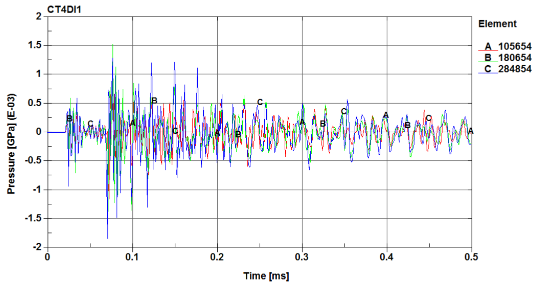

(a) *Penalty based constraint, compression and tension*

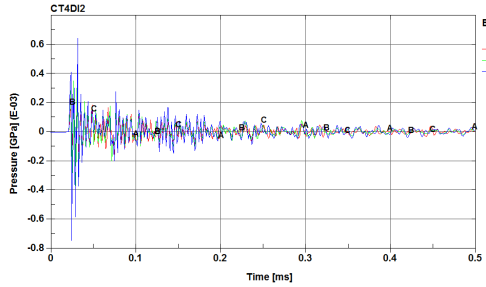

(b) *Penalty based constraint, compression*

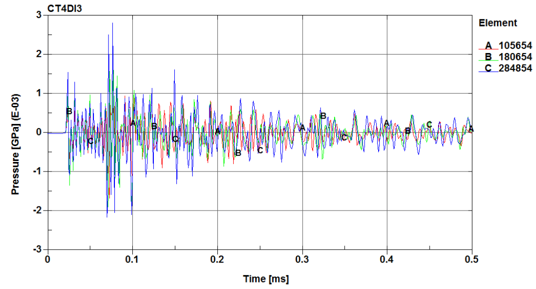

(c) *Penalty based constraint, all directions*

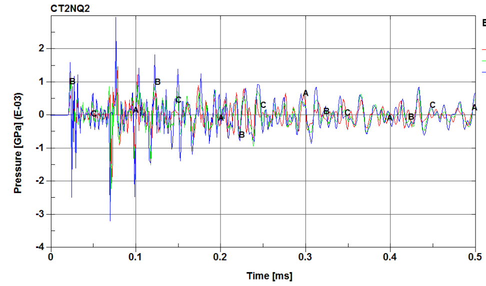

(d) *Velocity and acceleration constraint*

Figure 4.3: *Unfiltered Pressure measurements , [ms] vs [GPa]*

To compare with the filtered results from the experimental testing, the simulated pressures were filtered (see Figure 4.4), as in the experiments, using a Butterworth filter function, at 10 kHz.

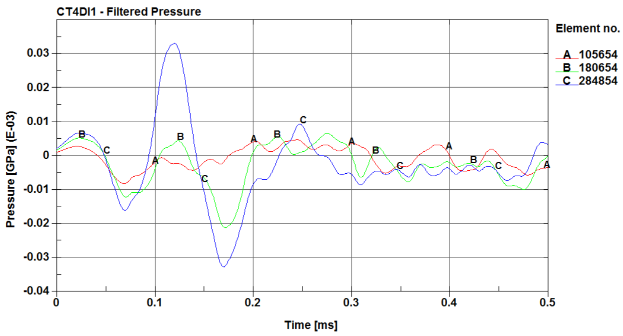

(a) *Penalty based constraint, compression and tension*

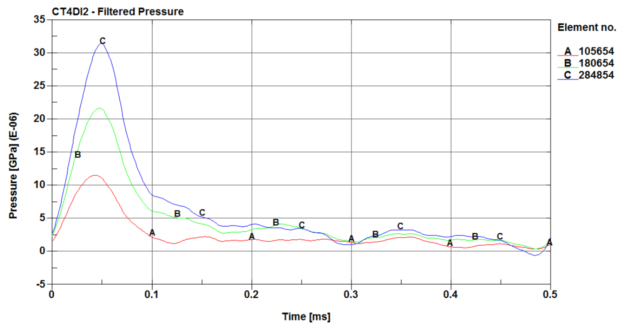

(b) *Penalty based constraint, compression*

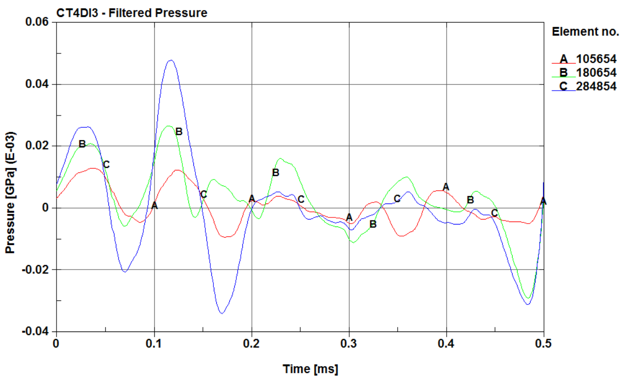

(c) *Penalty based constraint, all directions*

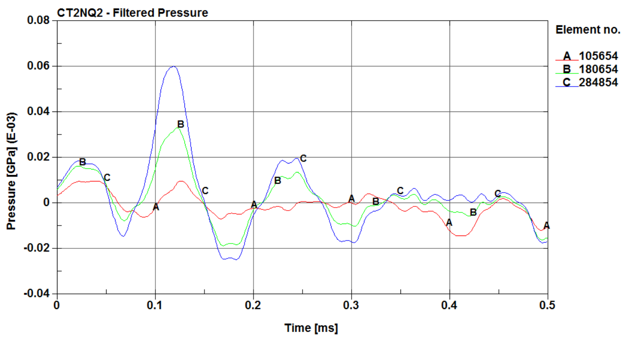

(d) *Velocity and acceleration constraint*

Figure 4.4: *Filtered pressure measurements from the gel simulations*

As expected based on the theory, the penalty based contact in compression shows the most accurate pressure distribution, see Figure 4.4b. Further images of the gel distribution with different bolt contacts can be found in Appendix A. The number of coupling points were set to three, which thereby added three points of spring force between the elements.

As in the experiments the largest pressure is recorded in the element at a 0° angle from the bolt.
When increasing the bolt velocity to the approximate levels of the physical tests the results show an even clearer similarity to the experimental results, see Figure 4.5. The central measurements reach the highest levels, indicating that the angle of penetration is important in the distribution of the pressure.

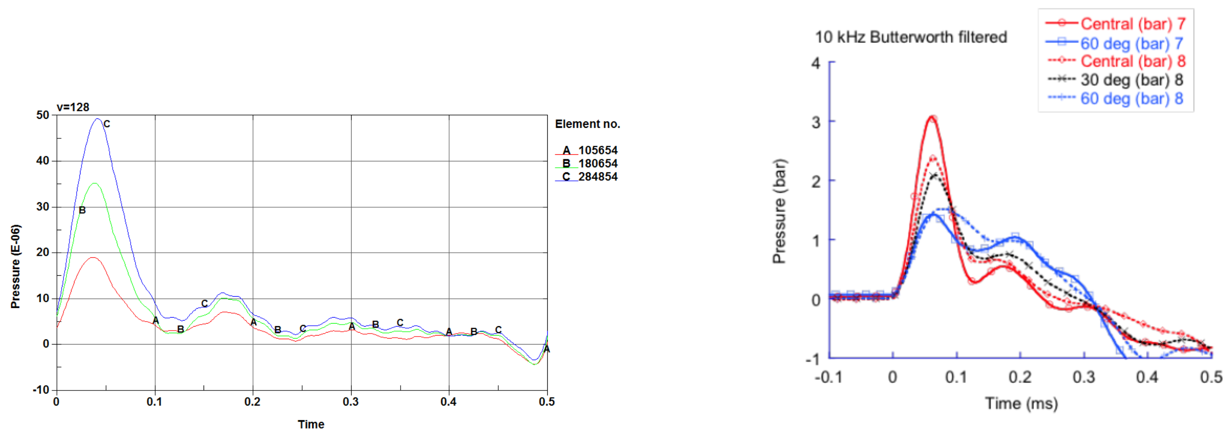

(a) *Penalty based constraint, compression and tension*

(b) *Penalty based constraint, compression*

Figure 4.5: *Pressure comparison with experimental results, [ms] vs [GPa], (1 bar=* 10^{-4} *GPa)*

The levels of the pressure are not precisely the same. The simulated pressure reaches it's maximum level at approximately 0.5 bar when increasing the bolt velocity to 128 m/s, differing by a factor of 6 from the experimental level of approximately 3 bar. Some of the negative pressure has not been reached in the simulated results. This as a possible effect of the lack of a collapsible cavitation, according to Zhang et al [10].
This was deemed an adequate model to determine which parameters to use in the final brain modeling.

4.2 FE Rat Brain pressures

Based on the results from the gel model, the contact between the skull and the tissue was chosen as Ctype 4 with Direc 2. So was the contact between the bolt and the tissue, and between the bolt and the voids. As for the gel model, the bolt was given a velocity for a fixed amount of time, until reaching the required depth. All other movements were locked, and the bolt was held fixed in space after the movement ended. After the bolt penetration there was, as in the gel model, an increased stress around the bolt. According to Figure 4.6 the material around the bolt penetration path was also pushed away. Some material was moved into the void, or mixed with other regions in the brain model.

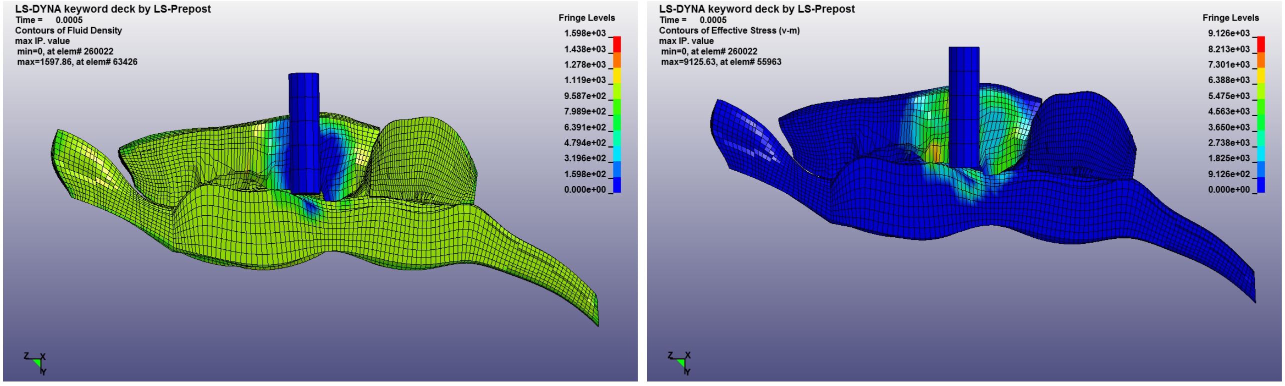

(a) *Fluid density after bolt penetration*

(b) *Effective von Mises stress, Pa, after penetration*

Figure 4.6: *Bolt position after movement*

In the elements established in Figure 3.6, the pressure was evaluated. The pressure is compared to the experimental pressures in the contra lateral ventricle for three different experiments, number 335, 336 and 337. After filtering with a Butterworth 10 kHz filter, the pressure from the advanced brain tissue model behaved according to Figure 4.7. Further pressure measurements are found in Appendix B.

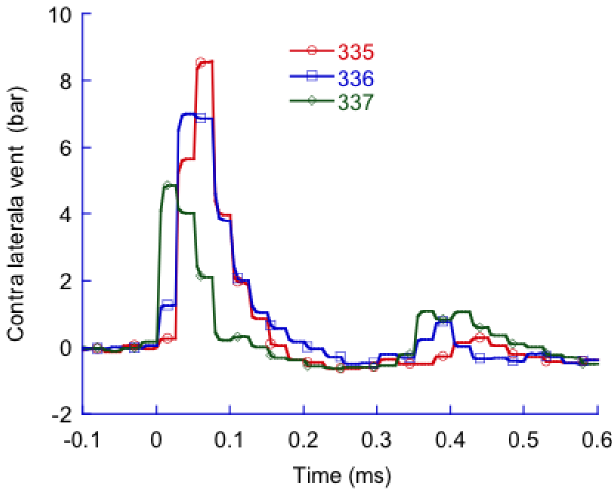

(a) *Experimental levels of pressure in the contra lateral ventricle for experiment 335, 336, 337*

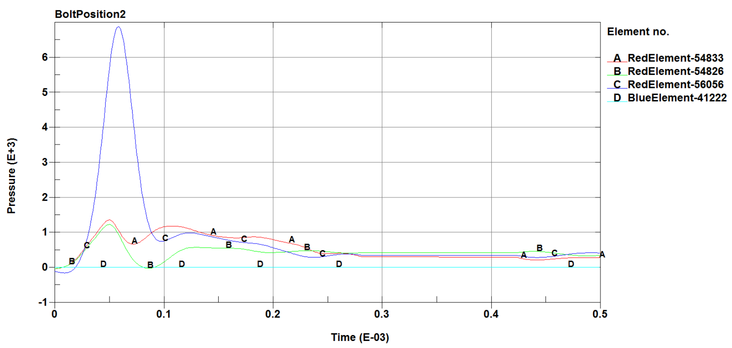

(b) *Simulated pressure in measuring elements*

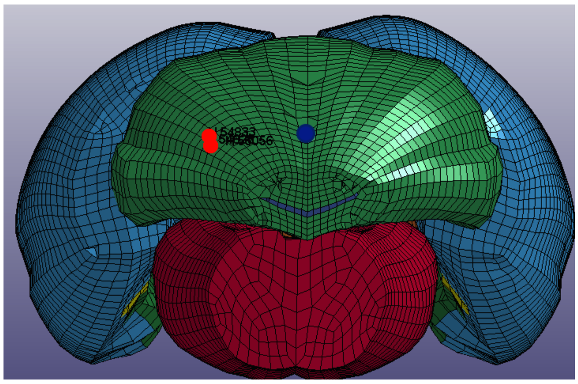

(c) *Position of measuring elements*

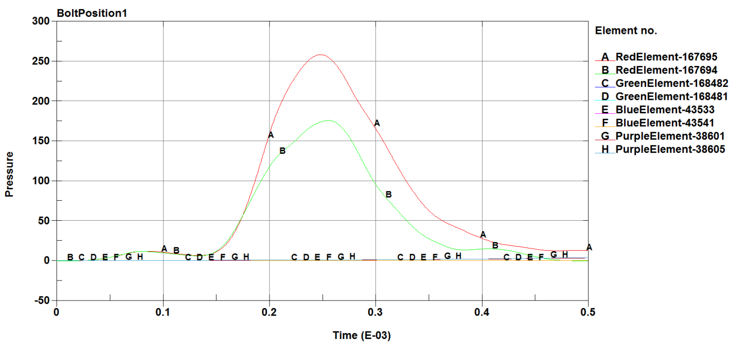

(d) *Simulated pressure in measuring elements*

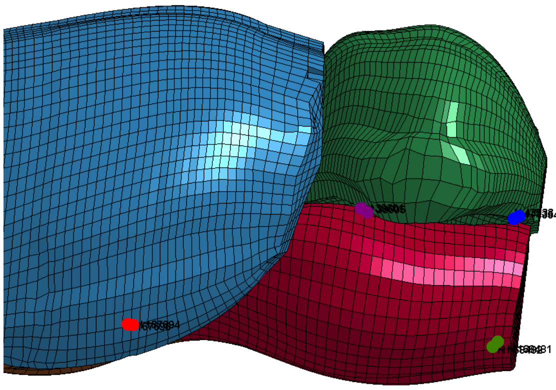

(e) *Position of measuring elements*

Figure 4.7: *Filtered pressure in simulations, [s] vs [Pa], compared to experimental pressure.*

Not all measuring positions gave reliable results. This is because in a physical rat brain, the distances between the brain regions are minimal, whereas in the rat brain FE model the different brain regions have rather large distances between them. This creates empty spaces where in reality a tissue exists, enabling transference of the pressure. Therefore only regions of the brain that have zero or small distances between the brain regions are chosen as reliable enough for measurements. This means that the only comparable results come from the sensors in the contra lateral ventricle, meaning the red elements in figure **??**.

4.3 Varying of External Parameters

To establish a pattern in the behavior of the pressure, the external variables were modified. A primary set of simulations were performed, wherein the bolt was moved anterior, and then posterior, to its initial position, (see Figure 4.8). The timestep, DT, was set to 10^{-5} ms.

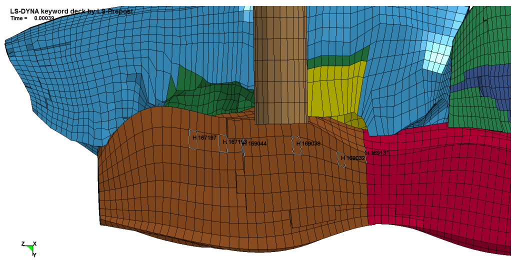

(a) *Original position of bolt*

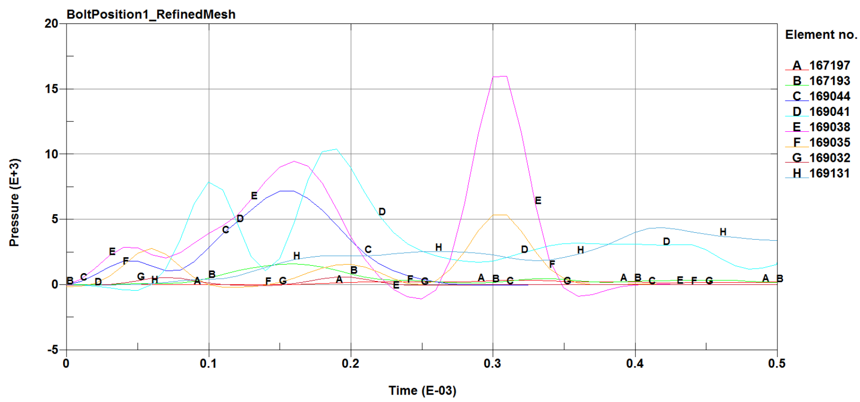

(b) *Pressure in chosen elements*

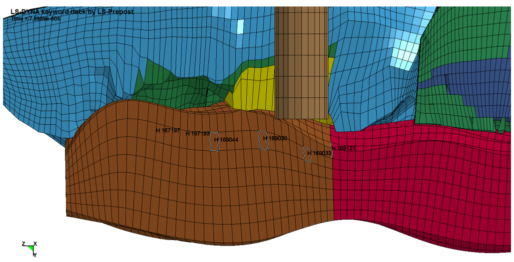

(c) *Bolt position back 2mm*

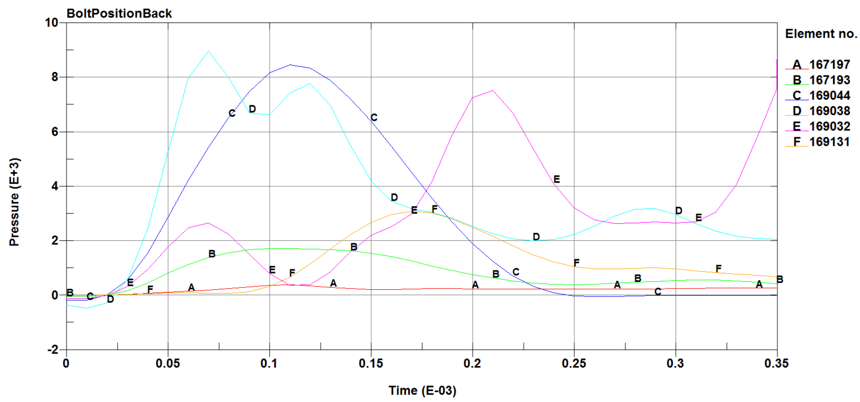

(d) *Pressure in chosen elements*

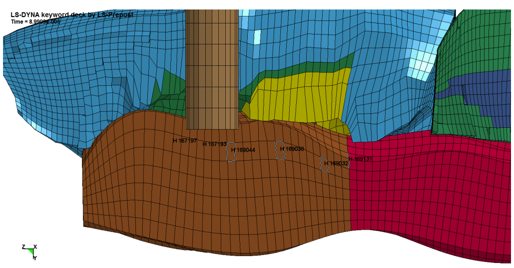

(e) *Bolt position forwards 2mm*

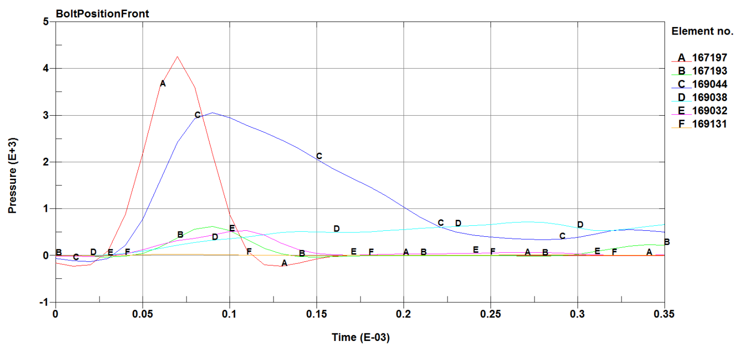

(f) *Pressure in chosen elements*

Figure 4.8: *Pressure, [s] vs [Pa], measured when altering the position of the bolt*

Most of the results seemed to be in agreement with the theory that the peak pressure will be reached at a position directly in front of the bolt. Some differences were found, as in Figure 4.8d, where the highest and earliest pressure are not in the bolts path. This was probably caused by the lack of material in that specific region. The area with the peak pressure was in a part of the model where there were no gaps of material, enabling the pressure to travel ahead of the bolt.

In Figure 4.8f the pressure has been able to travel directly in the path of the bolt all the way down to the measuring points, because of the consistency of the material distribution.
A secondary simulation varied the angle of the bolt impact, see Figure 4.9. The timestep was set to 10^{-6} ms.

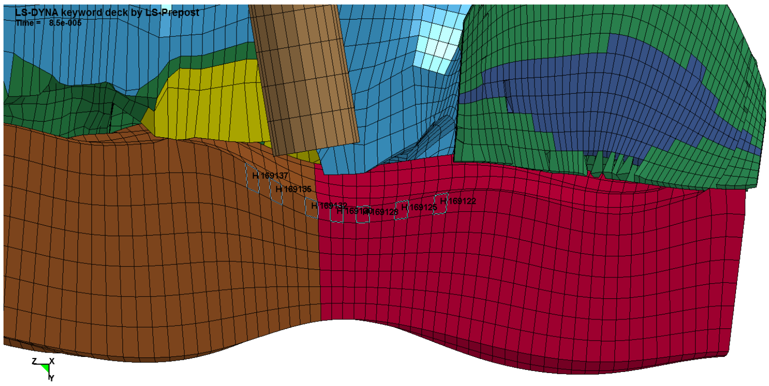

(a) *Elements and bolt when bolt is angled 10 degrees from the y-axis*

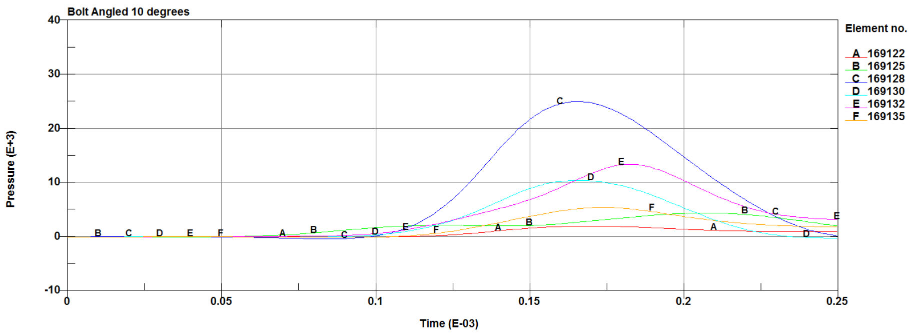

(b) *Pressure in chosen elements with a 10 degree angle*

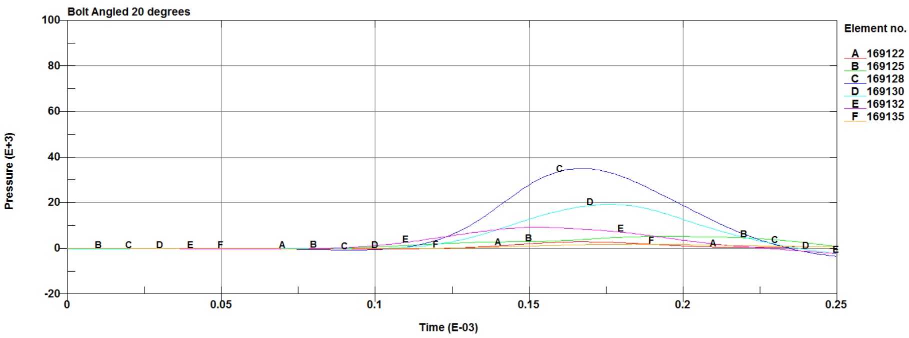

(c) *Pressure in chosen elements with a 20 degree angle*

Figure 4.9: *Pressure measured when altering the position of the bolt, [s] vs [Pa]*

When angleing the bolt by 10° and then 20 ° from the y-axis the pressure distribution did not change dramatically. However, the levels of the pressure changed. The elements that got a position more directly in the path of the bolt, in Figure 4.9c, got a higher peak pressure than when they were slightly offset from the path, as in Figure 4.9b.
The angle and position of the bolt clearly affect the pressure.

5 Discussion

The comparison between the simple gel test simulations and the gel experiments worked well. Although only two of the physical experiments were deemed reliable, the simulated pressure displayed a very similar behavior.

Because of the number of error sources in the original experiments, there was no focus put on establishing a more accurate result. It is clear that the contacts between the modeled parts have a large affect on the results, so the simplifications made between the gel and the casing is a possible error source. Further simplifications such as the modeling of the casing could also be found to affect the pressure measured.
The discrepancies between physical experiments and simulations may have a number of sources. For instance the measurements in the FE-model were taken at the elements corresponding to the position of the pressure probes, while not modeling an actual probe. The pre-drilled hole through the plate was round in the experiments, while limitations in the CAD process meant that it was simplified as a square hole in the model. The casing around the gel was not actually an immovable rigid material, but a plastic that could take some slight deformation. The bolt penetration depth in the experiments were meant to be 5 mm but varied between 5.8-6.9 mm. Only the last two of the physical experiments were judged as reliable.
In the gel test simulations it became clear that the speed of the bolt had a very large impact on the peak pressure. This is what was expected to be found. In the modeling it is clear that the density of the material is a very large factor in the pressure behavior. This is not a variable that is possible to change in reality, but it is however important for the improvement of the modeling.

Because of the original modeling of the RBM, directly comparable results between the experiments and the simulations are not found. The levels of the simulated pressures does not correspond to the levels found in the experiments. In the original simulation the peak pressure is around 8000 Pa, or 0.08 bar. In the physical experiments the peak pressures are found around 8 bar. This is a difference of about a factor 100. However the general shape of the pressure plot indicate that the setup may not be completely flawed. The boundary conditions of the skull and neck were greatly simplified for the sake of the simulation. The main cause of the discrepancies is believed to be in the modeling of the RBM. The original RBM was created to investigate rotational trauma, where the gaps in between the brain regions may not have an affect. However, when searching for a realistic transfer of pressures, the gaps become very problematic. There is also a significant distance between the brain tissue and the skull that is not realistic and may cause the much lower pressure measurements.
The simulations performed when varying the external parameters of the bolt, are seen as very positive. The peak pressure is increased to around 15000 Pa, or 0.15 bar. It seems clear that the path uninterrupted by gaps yields the highest pressures. This is a further indication that the discrepancies between the physical results and the simulations are exacerbated by the empty areas between brain regions.
The simple translation of the bolt backwards or forwards greatly changed the results. However, since the repositioning put the bolt in paths across different gaps of material, these measurements alone would not be reliable. The results from the angeling of the bolt is a strong indication that any angle change will affect the pressure in the regions dramatically.
Some of the differences in the simulated pressure output, when comparing to the physical test, may be caused by the lack of a modeled sensor. Elements were chosen at the sensor measuring points, but no modeling of a simulated sensor was performed. Since pressure is very affected by reflection off surfaces, this may be causing some of the discrepancies. There are smaller error sources as well, such as the simplifications of the experimental setups.
In the RBM the bolt was controlled as to reach a depth of 6 mm into the brain tissue. In the physical test the bolt penetration varied between 5.8-6.9 mm.
The RBM mesh is still not fine enough to give a completely reliable result. To find a stable pressure propagation the mesh has to be extremely fine. The ALE method is less mesh-size dependent than the Lagrange method, but would still probably require some further mesh refinement.
The voids around the brain tissue are not completely optimal. The void elements created became rather large, but further refinement was outside the scope of this thesis.

6 Conclusions

The speed, position and angle of the bolt penetration strongly affect the pressure behavior. Based on this, a change to the cattle stunning procedure could have a great affect on the stun quality. This would of course be dependent on the size of the region which is targeted. It is not certain that the results found in the rat brain model are simply a scaled down version of of the pressure in larger animals. A stiffer neck, a thick skull and a change of tissue parameters may change the behavior of the pressure from the results presented here.

6.1 Recommendations for further work

There are a number of possible error sources that could be eliminated through future work. The most clearly detected error sources are the gaps in between the brain regions. These could possibly be eliminated by an expansion of the RBM, or by filling the spaces with a temporary material, corresponding to the brain material. This should enable a more clear transfer of forces and pressures in between the regions. The gap between the brain and the skull should also be eliminated, since the tissue should be restricted by the skull and not be able to move. To establish a completely reliable model, a mesh refinement would be necessary. A refinement of the void meshes would also be beneficial. Boundary conditions should be investigated further, as well as contacts, since they have a strong affect on any simulation.

References

[1] Hallelujah Acres *The Brain & Your Nervous System.* http://www.hacres.ca/wp-content/uploads/2014/06/the-brain.jpg, 2014-09-09

[2] Liu, L & Fan,Y & Li,W 2014 *Viscoelastic Shock wave in ballistic gelatin behind soft body armor.* Zhejiand Universty, Hangzhou 310027, P.R. China

[3] Krave, U 2010, *Modelling of Diffuse Brain Injury: Combining Methods to Study Possible Links between Transient Intracranial Pressure and Injury.* Chalmers University of Technology, Göteborg, Sweden.

[4] Wittek, A & Omori, K 2003, *Parametric Study of effects of Brain-Skull Boundary Conditions and Brain Material Properties on Responses of Simplified Finite Element Brain Model under Angular Acceleration Impulse in Sagittal Plane.* Toyota Central R&D Labs. Inc, Nagakute, Japan.

[5] Kleiven, S & von Holst H 2002, *Consequences of head size following trauma to the human head.* Journal of Biomechanics 35, pp. 153-160.

[6] Pearce, C & Young, P G, & Cowlam, L & Walker, B 2013 *The pressure response in the brain during short duration impacts.* University of Exeter, Exeter, UK

[7] Deck, C & Willinger, R 2009 *The current state of the human head finite element modelling.* Strasbourg Universitym UdS-IMFS CNRS, Strasbourg, France

[8] Brands, DWA 2002 *Predicting brain mechanics during closed head impact.* Technische Universiteit Eindhoven, Eindhoven, The Netherlands.

[9] Chafi, MS, Karami G & Ziejewski, M 2010, *Biomechanical assessment of Brain Dynamic Responses Due to Blast Pressure Waves.* Annals of Biomedical Engineering, Vol. 38, No 2, pp.490-504.

[10] Zhang, J & Yoganandan, N & Pintar, F A & Gennarelli, T A 2005 *Temporal Cavity and Pressure Distribution in a Brain Simulant following Ballistic Penetration.* Journal of Neurotrauma, Volume 22, Number 11, 2005, pp. 1335 - 1347

[11] Zhu, F & Wagner, C & Dal Cengio Leonardi, A & Jin, X & Vande Vord, P & Chou, C & Yang, K H, & King, A I 2011 *Using a gel/plastic surrogate to study the biomechanical response of the head under air shock loading: a combined experimental and numerical investigation.* Bioengineering Center, Wayne State University, Detroit, USA

[12] Bradshaw, DRS & Morfey, CI *Pressure and Shear Responses in Brain Injury Models.* University of Southampton, UK.

[13] Antona-Makoshi, J, Davidsson, J, Risling, M, Ejima, S & Ono, K 2013, *Validation of local brain kinematics of a novel rat brain finite element model under rotational acceleration and its application towards the clarification of Diffuse Axonal Injury mechanisms.* JSAE Annual Congress.

[14] Deck, C & Willinger, R 2009, *Head injury prediction tool for protective systems optimisation.* Strasbourg University, IMFS-CNRS, Strasbourg, France.

[15] Patel, A & Goswami, T, *Comparison of Intracranial Pressure by Lateral and Frontal Impacts - Validation of Computational Model.* Wright State University, Dayton, USA.

[16] Zhu, F & Mai, H & Dal Cengio Leonardi, A & Wagner, C & Chou, C & Jin, X & Bir, C & Vande Vord, P & Yang, K H, & King, A I 2010 *Development of an FE Model of the Rat Head Subjected to Air Shock Loading.* Stapp Car Crash Journal, Vol. 54, pp. 211-225

[17] Gupta, RK & Przekwas, A 2013 *Mathematical models of blast-induced TBI: current status, challenges, and prospects.* Frontiers in Neurology , Vol. 4, article 59.

[18] Fijalkowski, RJ & Yoganandan, N & Zhang, J & Pintar, F A 2009 *A Finite Element Model of Region-Specific Response for Mild Diffuse Brain Injury.* Stapp Car Crash Journal, Vol. 53, pp. 193-213

[19] Deck, C & Willinger, R 2009, *Improved Model based Head Injury Criteria*. Strasbourg University, IMFS-CNRS, Strasbourg, France.

Appendix

Appendix A

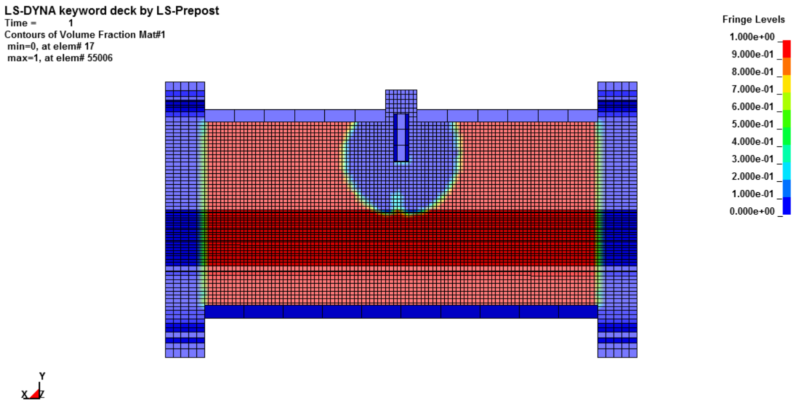

(a) *Ctype 4 with Direc 3*

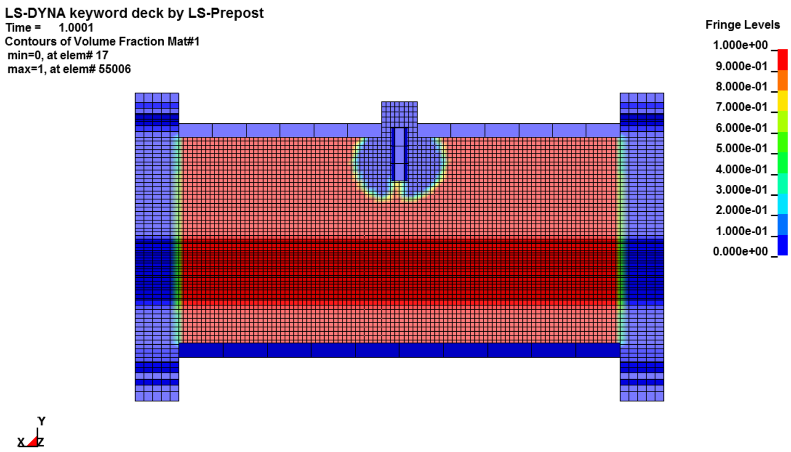

(b) *Ctype 4 with Direc 1*

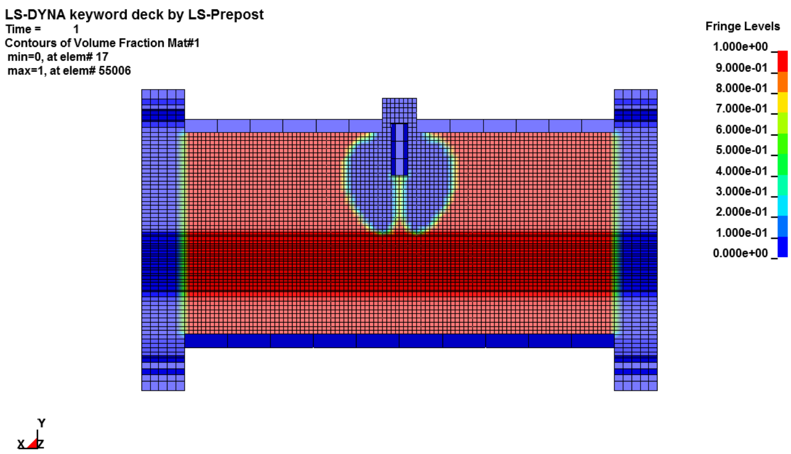

(c) *Ctype 2*

Figure 6.1: *Gel movement when altering the contact definition between bolt and gel*

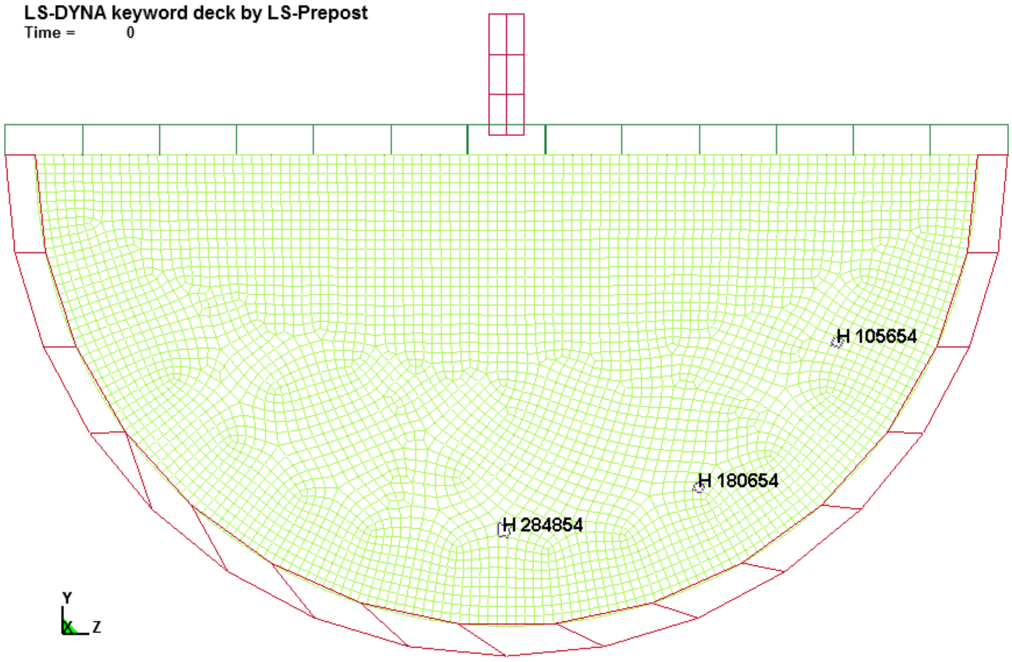

Figure 6.2: *Measuring elements for data extraction*

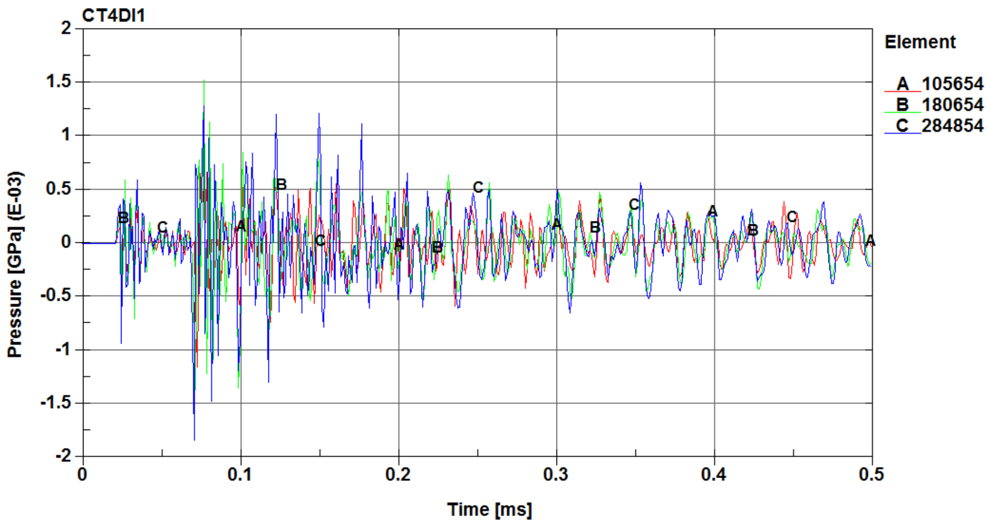

(a) *Penalty based constraint, compression and tension*

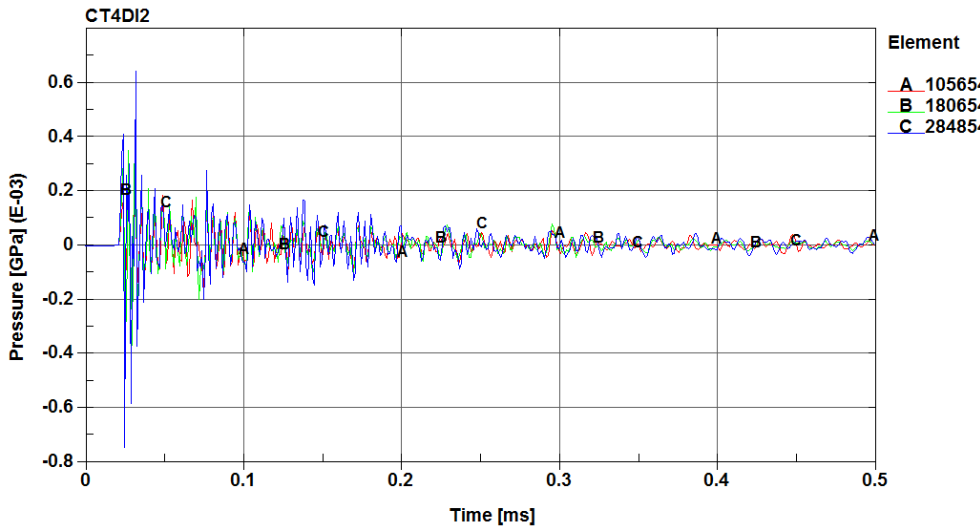

(b) *Penalty based constraint, compression*

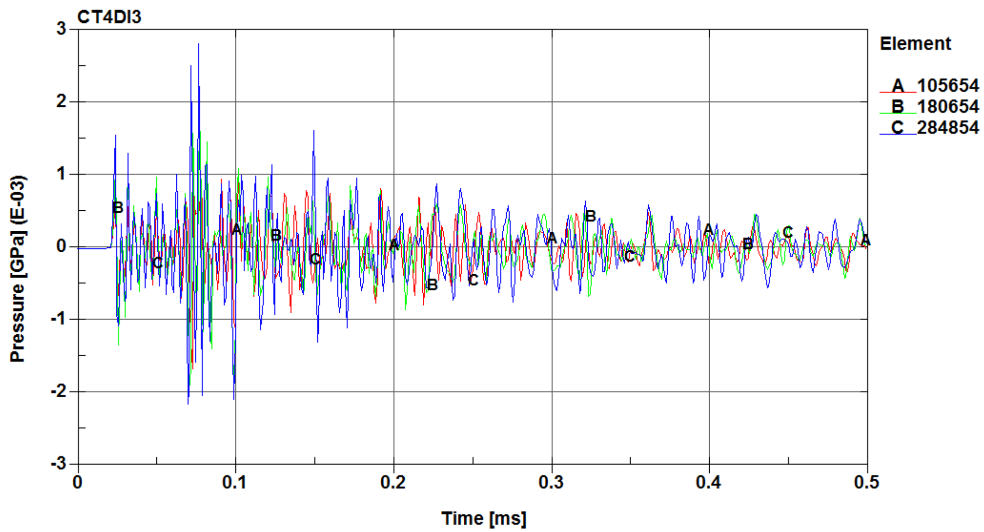

(c) *Penalty based constraint, all directions*

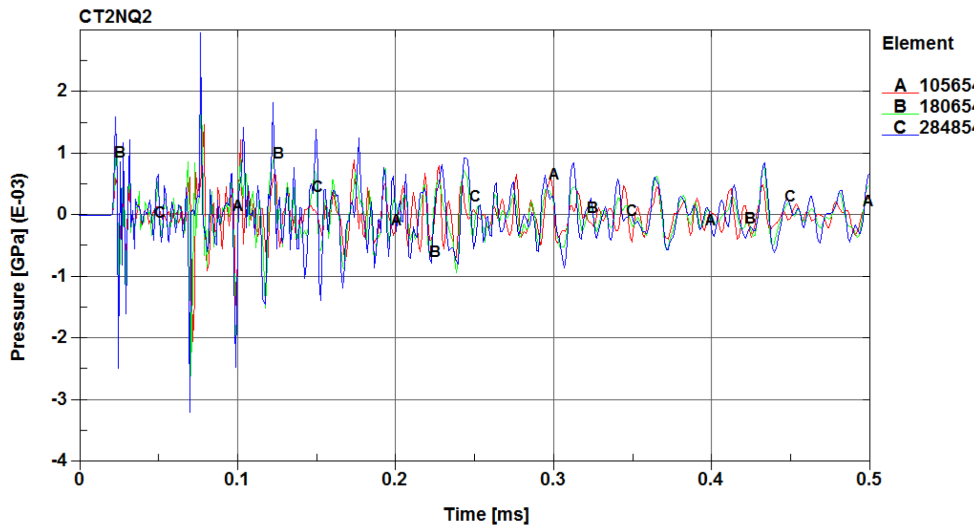

(d) *Velocity and acceleration constraint*

Figure 6.3: *Simplified model pressure*

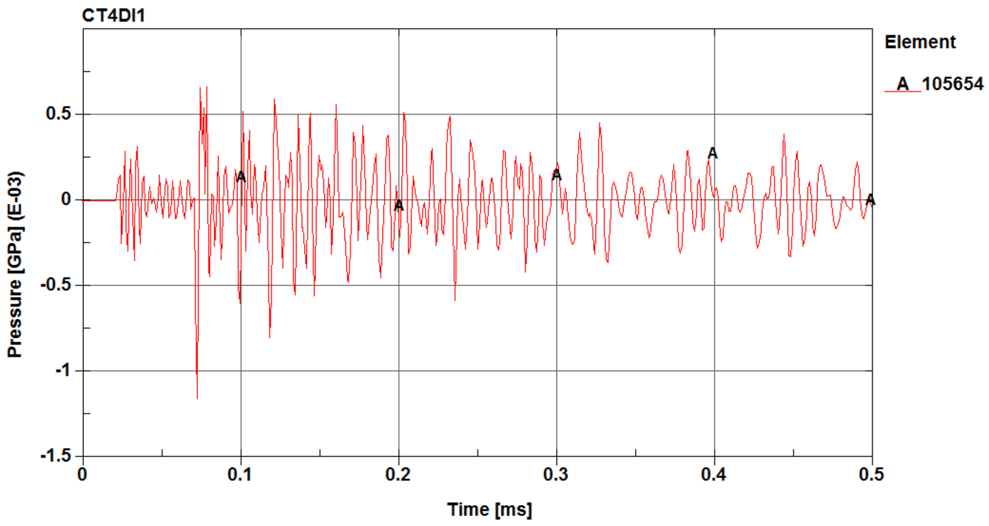

(a) *Penalty based constraint, compression and tension*

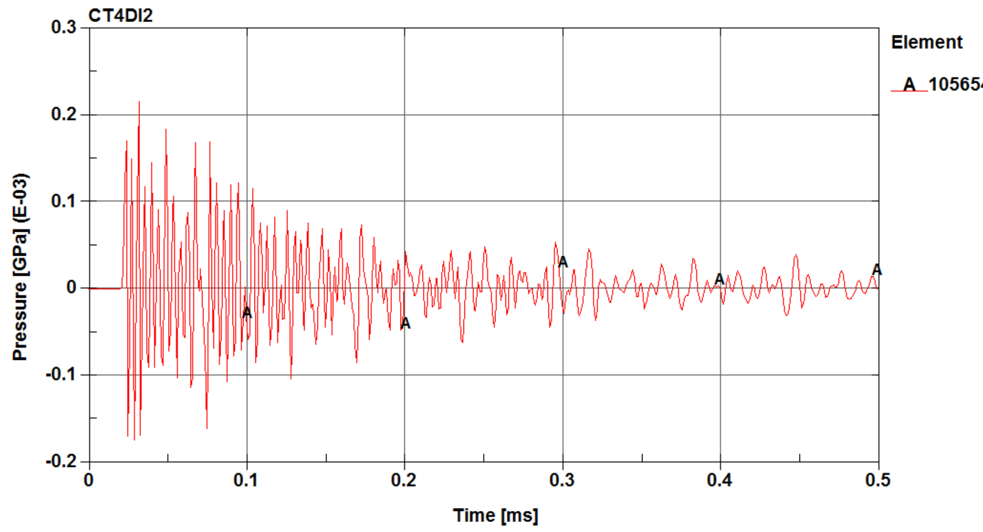

(b) *Penalty based constraint, compression*

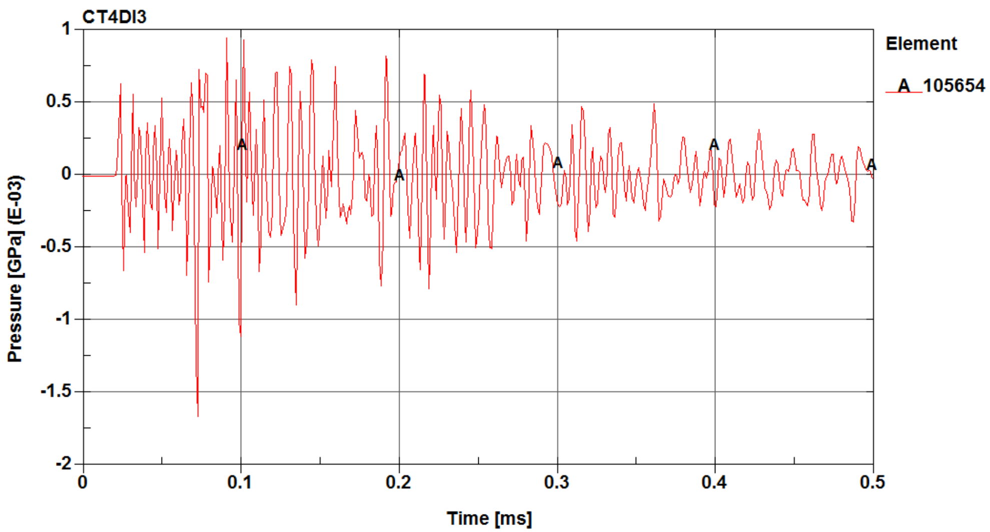

(c) *Penalty based constraint, all directions*

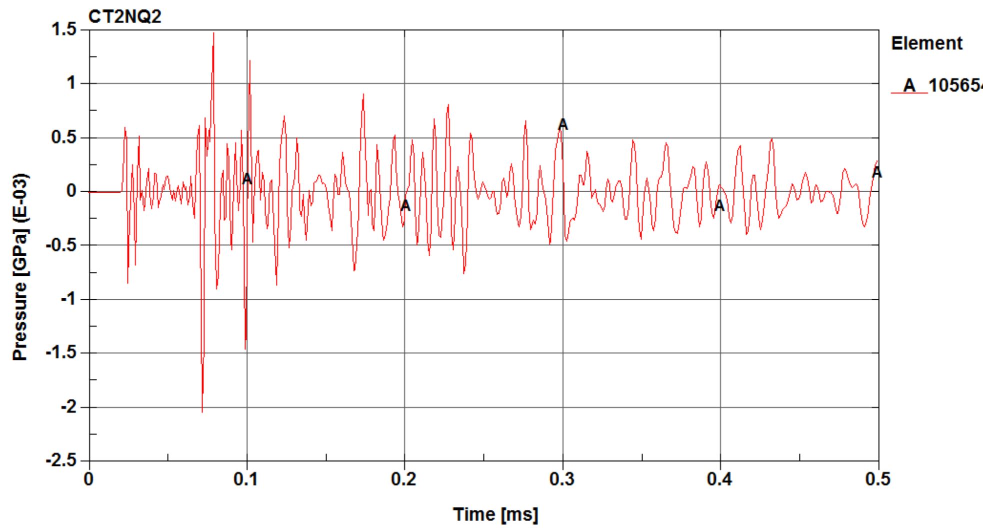

(d) *Velocity and acceleration constraint*

Figure 6.4: *Simplified model pressure at 60 degrees*

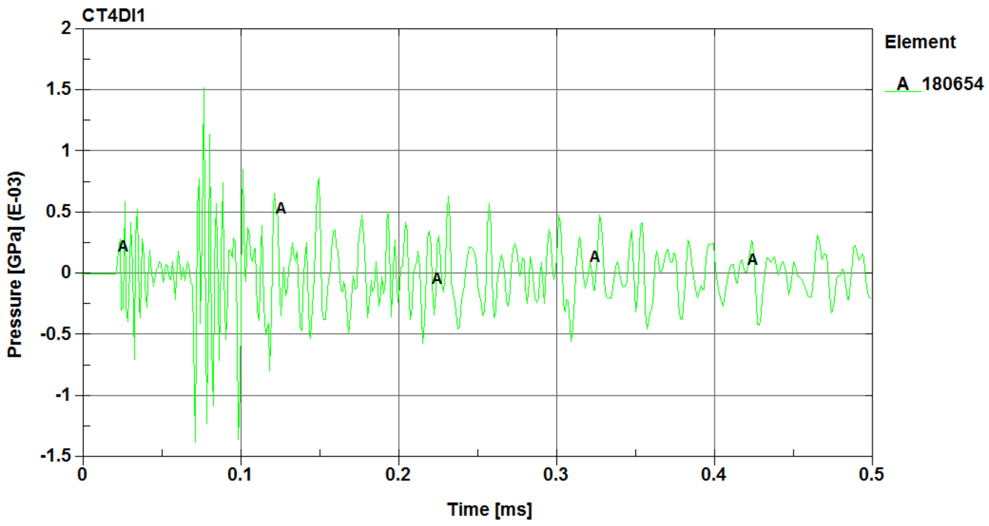

(a) *Penalty based constraint, compression and tension*

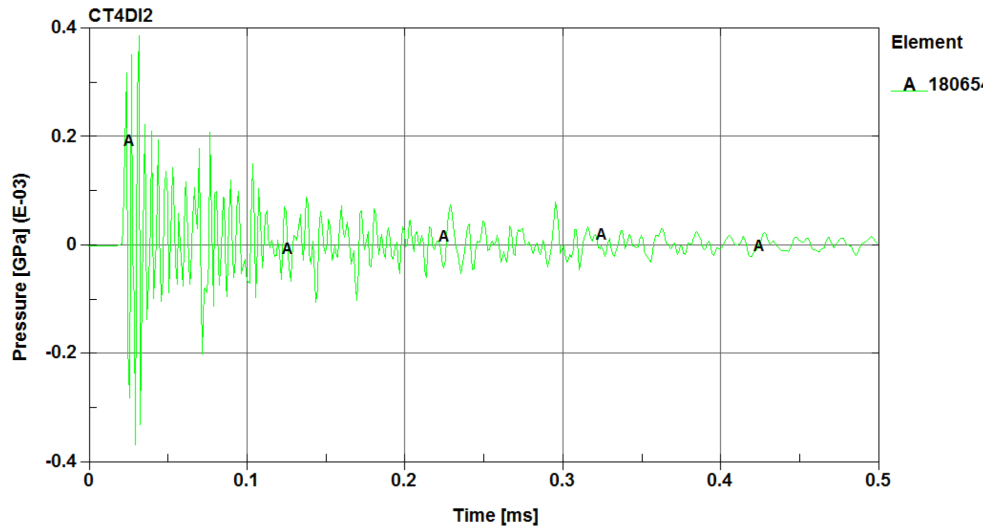

(b) *Penalty based constraint, compression*

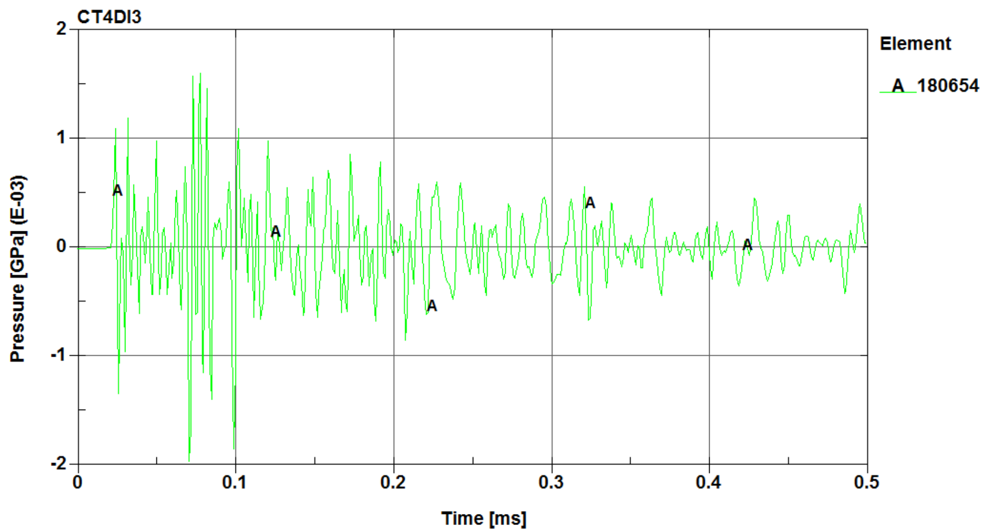

(c) *Penalty based constraint, all directions*

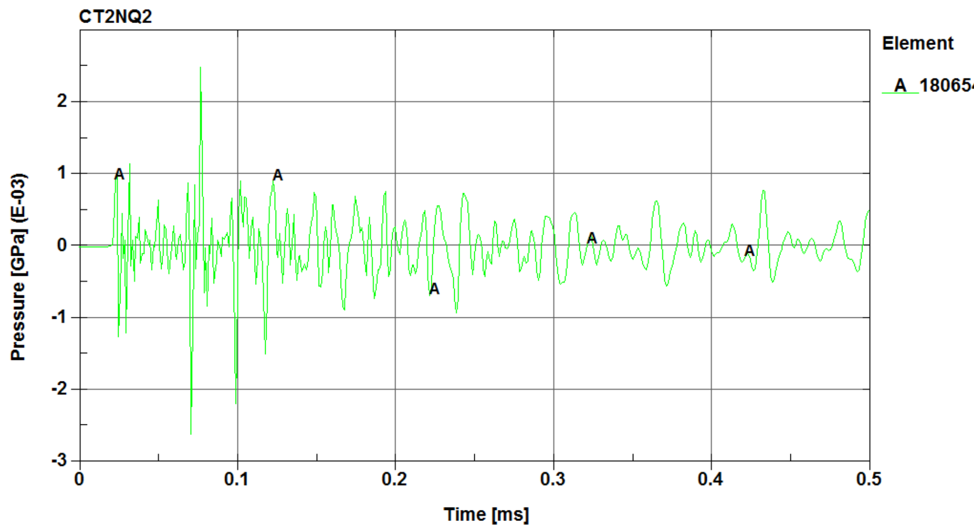

(d) *Velocity and acceleration constraint*

Figure 6.5: *Simplified model pressure at 30 degrees*

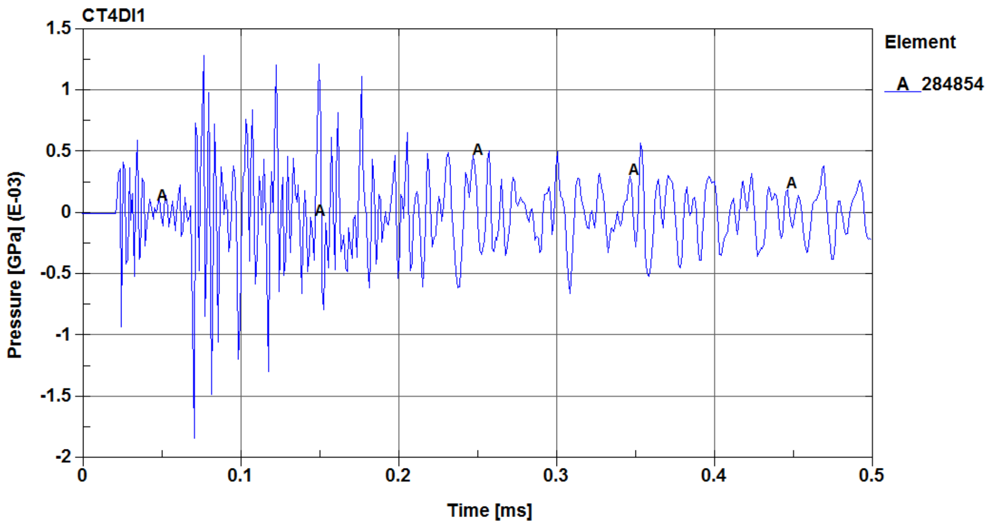

(a) *Penalty based constraint, compression and tension*

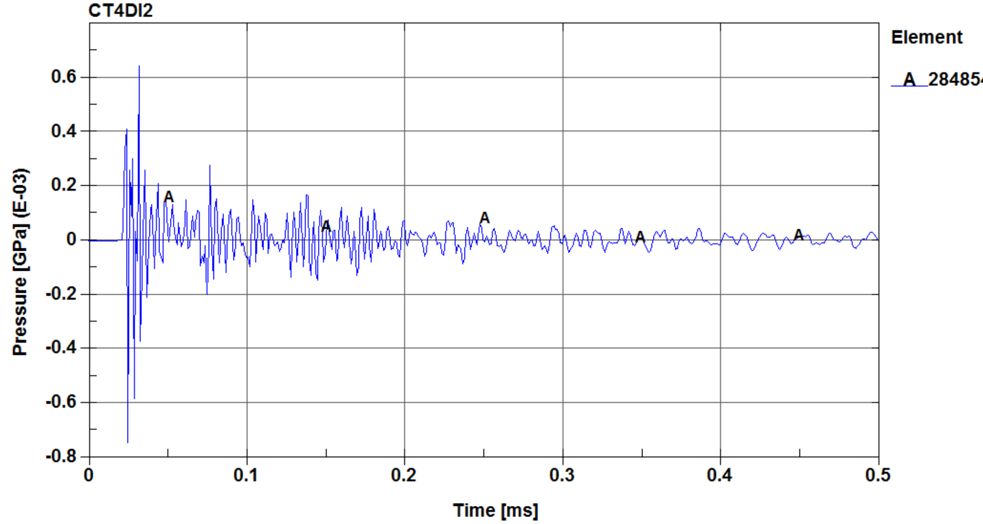

(b) *Penalty based constraint, compression*

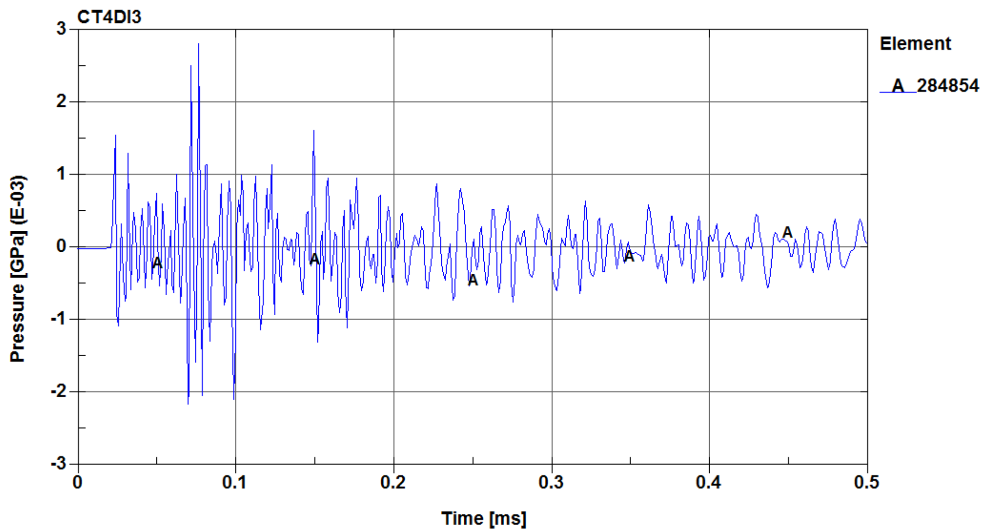

(c) *Penalty based constraint, all directions*

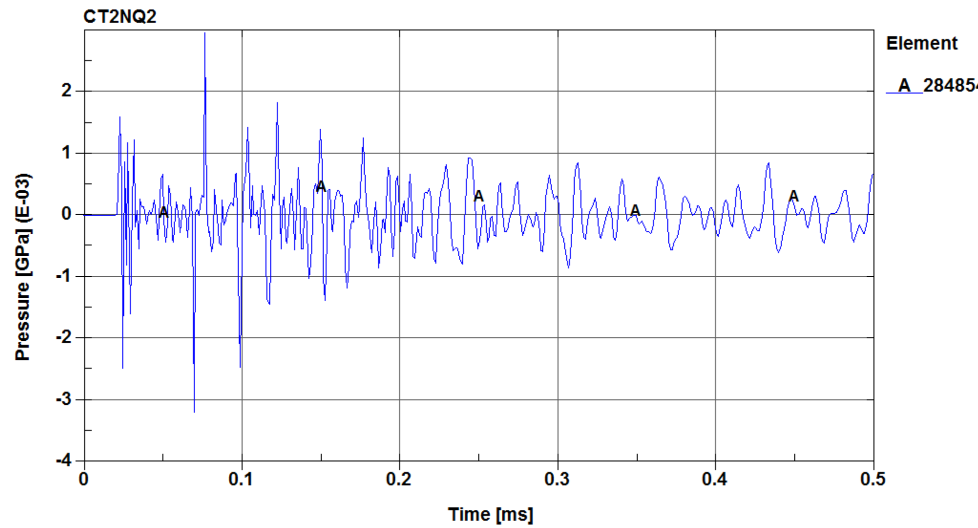

(d) *Velocity and acceleration constraint*

Figure 6.6: *Simplified model pressure at 0 degrees*

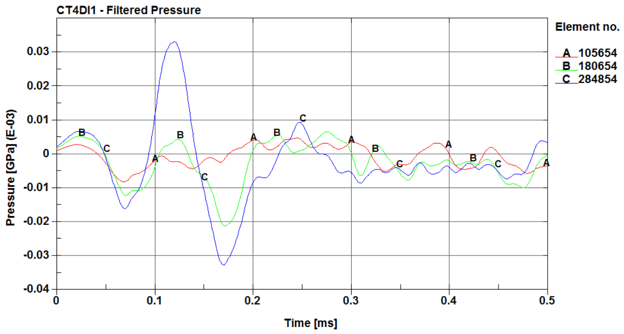

(a) *Penalty based constraint, compression and tension*

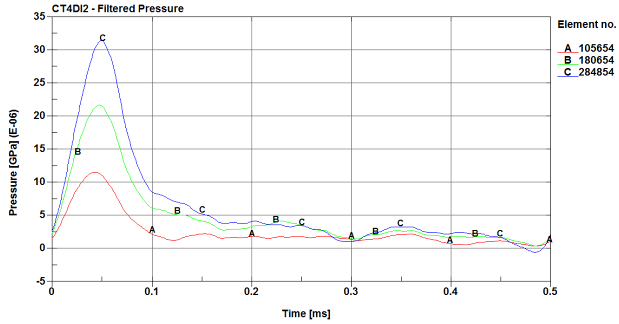

(b) *Penalty based constraint, compression*

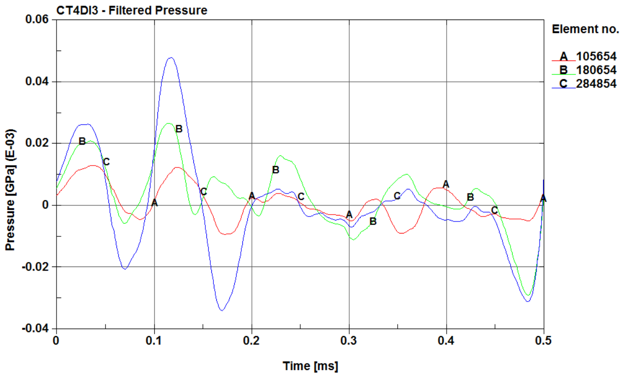

(c) *Penalty based constraint, all directions*

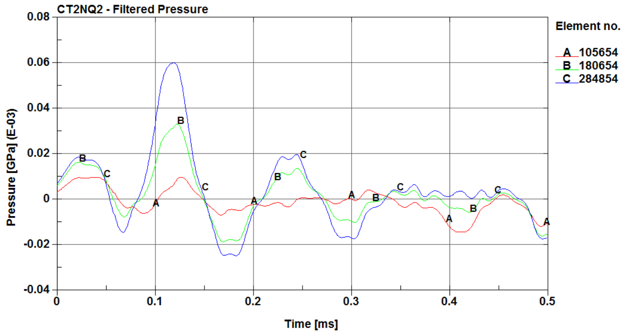

(d) *Velocity and acceleration constraint*

Figure 6.7: *Filtered pressure from simplified model*

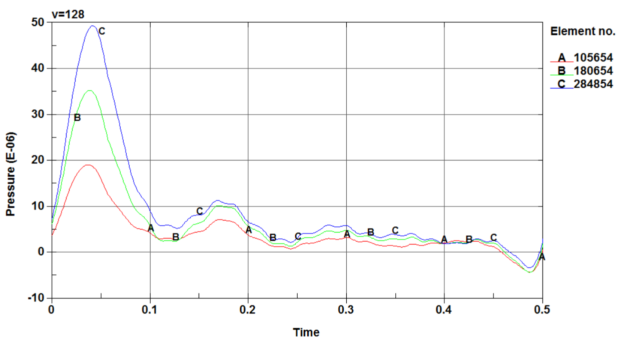

(a) *Penalty based constraint, compression and tension*

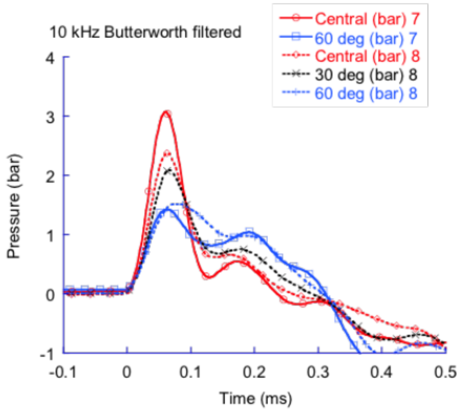

(b) *Penalty based constraint, compression*

Figure 6.8: *Comparison with experimental results*

Appendix B

List of .k-files in the modified FE-model:
main.k
GeneralControlDatabase.k
RatHead_v1_140403_Geometry_mod.k
RatHead_v1_140403_NoGeometry.k
BoundaryConditions.k

	G∞[Pa]	G1	τ1	G2	τ2	G3	τ3
Brainstem & Spine	240	1387	0.012	353	0.160	217	2.75
Cerebellum Grey	189	1391	0.009	353	0.226	240	5.37
Cerebellum White	169	1308	0.011	347	0.193	197	4.13
Corpus Callosum	208	1249	0.015	381	0.239	230	4.52
Hippocampus	528	1897	0.017	636	0.244	439	4.72
Cortex	433	1113	0.019	393	0.314	261	4.92
Thalamus & Bulbus olfactorius	347	1533	0.017	464	0.318	312	6.66

Figure 6.9: *Prony material parameters for RBM*

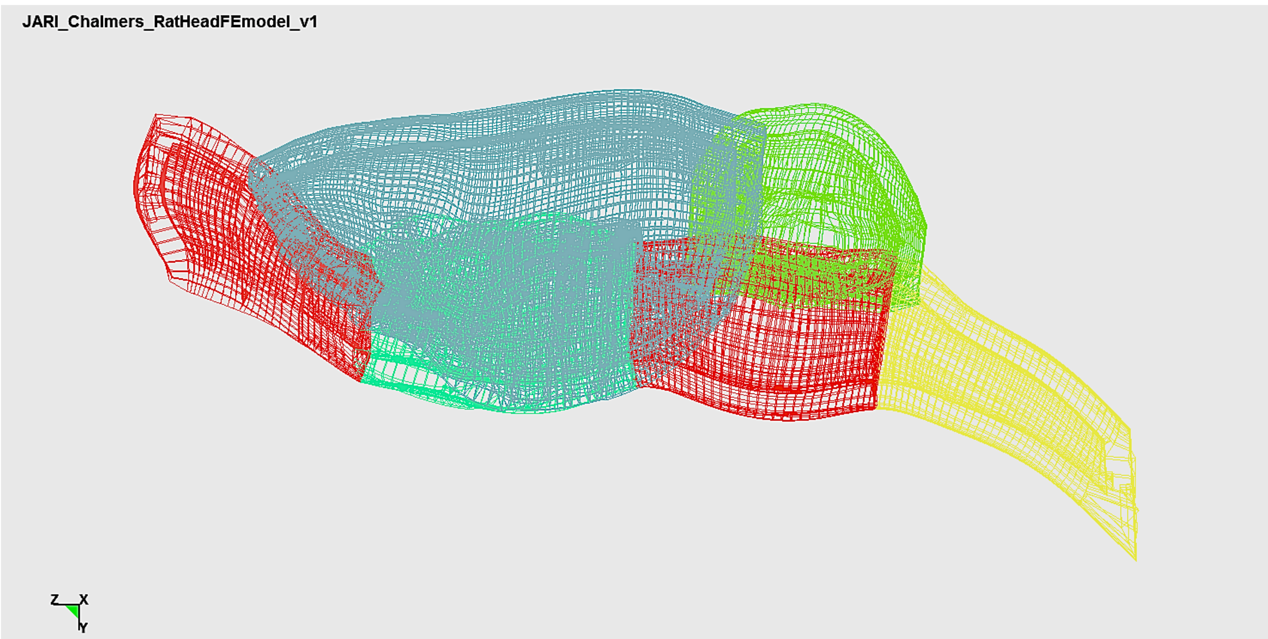

Figure 6.10: *Voids in RBM*

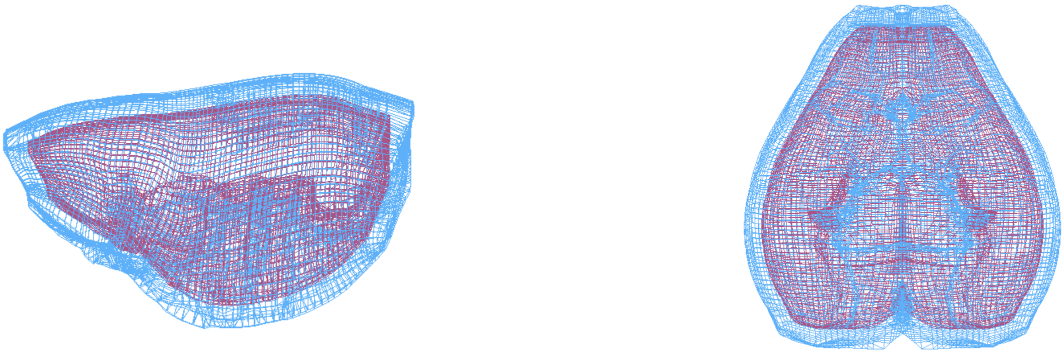

Figure 6.11: *Void surrounding the Cerebrum*

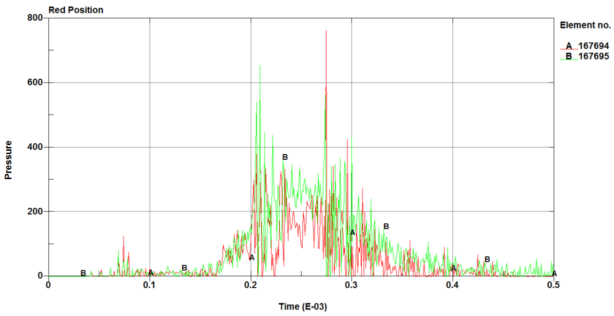

(a) *Red Sensor*

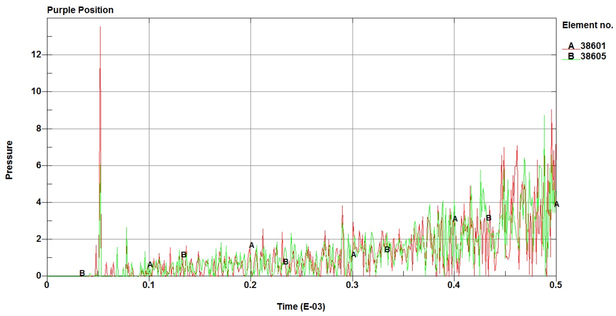

(b) *Purple Sensor*

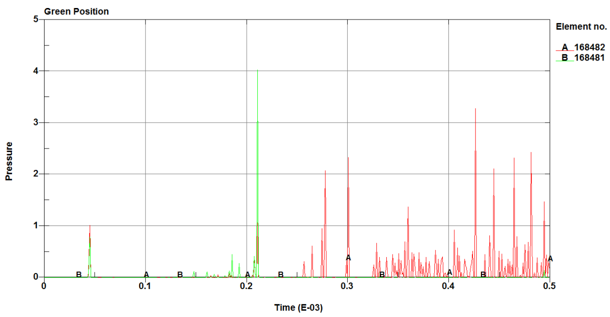

(c) *Green Sensor*

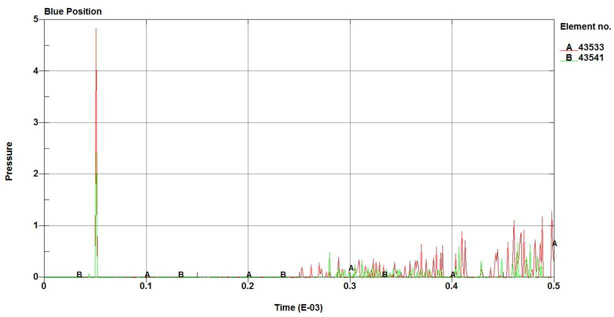

(d) *Blue Sensor*

Figure 6.12: *Pressure from RBM*

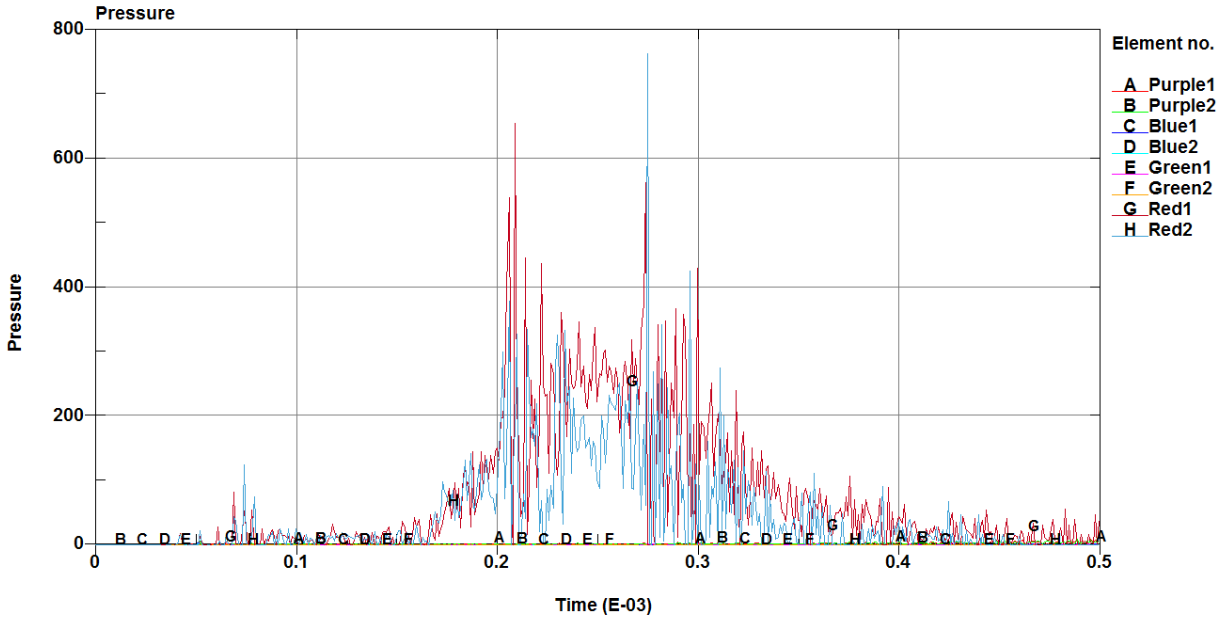

Figure 6.13: *Pressure from RBM - All sensors*

Appendix C

Relevant outtakes from the LS-DYNA keyword cards used in the simulations.

Gel test setup

```
$# LS-DYNA Keyword file created by LS-PREPOST 2.4 - 22Jun2009(14:31)
$# Created on Apr-01-2014 (09:09:29)
*KEYWORD
$$ Simulation Setup for GelTests
*TITLE
$# title
LS-DYNA keyword deck by LS-Prepost
*CONTROL_ALE
$#       dct      nadv      meth      afac      bfac      cfac      dfac      efac
           1         1         1  1.000000     0.000     0.000     0.000     0.000
$#     start       end     aafac     vfact      prit       ebc      pref   nsidebc
     0.0001.0000E+20  1.000000 1.0000E-6         0         0     0.000         0
*CONTROL_ENERGY
$#      hgen      rwen    slnten     rylen
           2         2         1         1
*CONTROL_TERMINATION
$#    endtim    endcyc     dtmin    endeng    endmas
    1.000000         0     0.000     0.000     0.000
*CONTROL_TIMESTEP
$#    dtinit    tssfac      isdo    tslimt     dt2ms      lctm     erode     ms1st
       0.000  0.700000         0     0.000     0.000         0         0         0
$#    dt2msf   dt2mslc     imscl
       0.000         0         0
*DATABASE_BINARY_D3PLOT
$#        dt      lcdt      beam     npltc    psetid
    0.015000         0         0         0         0
$#     ioopt
```

```
         0
*BOUNDARY_PRESCRIBED_MOTION_RIGID
$#     pid       dof       vad      lcid        sf       vid     death     birth
         6         2         0         1  1.000000         01.0000E+28     0.000
*BOUNDARY_SPC_NODE
$#     nid       cid      dofx      dofy      dofz     dofrx     dofry     dofrz
     58733         0         1         0         1         0         0         0
            .
            .
            .
       363         0         1         1         1         0         0         0
*CONTACT_AUTOMATIC_SURFACE_TO_SURFACE_ID
$#     cid                                                                 title
         1
$#    ssid      msid     sstyp     mstyp    sboxid    mboxid       spr       mpr
         6         1         3         2         0         0         0         0
$#      fs        fd        dc        vc       vdc    penchk        bt        dt
     0.000     0.000     0.000     0.000     0.000         0     0.0001.0000E+20
$#     sfs       sfm       sst       mst      sfst      sfmt       fsf       vsf
  1.000000  1.000000     0.000     0.000  1.000000  1.000000  1.000000  1.000000
*SET_PART_LIST_TITLE
Skal
$#     sid       da1       da2       da3       da4
         1     0.000     0.000     0.000     0.000
$#    pid1      pid2      pid3      pid4      pid5      pid6      pid7      pid8
        32         1         0         0         0         0         0         0
*PART
$# title
cylinder
$#     pid     secid       mid     eosid      hgid      grav    adpopt      tmid
         1         1         1         0         0         0         0         0
*SECTION_SOLID_TITLE
Solid
$#   secid    elform       aet
         1         1         0
*MAT_RIGID_TITLE
Rigid
$#     mid        ro         e        pr         n    couple         m     alias
         1 2.7000E-6 70.000000  0.350000     0.000     0.000     0.000
$#     cmo      con1      con2
     0.000         0         0
$# lco or a1       a2        a3        v1        v2        v3
     0.000     0.000     0.000     0.000     0.000     0.000
*PART
$# title
Bolt
$#     pid     secid       mid     eosid      hgid      grav    adpopt      tmid
         6         1         1         0         0         0         0         0
*PART
$# title
Gel
$#     pid     secid       mid     eosid      hgid      grav    adpopt      tmid
        26         2         2         0         0         0         0         0
*SECTION_SOLID_TITLE
ALE
$#   secid    elform       aet
```

```
         2        12         0
*MAT_VISCOELASTIC_TITLE
ViscoEl
$#     mid        ro      bulk        g0        gi      beta
         2 1.0400E-6  2.190000 1.7210E-6 5.0800E-7 215.00000
*PART
$# title
RVoid
$#     pid     secid       mid     eosid      hgid      grav    adpopt      tmid
        28         2         2         0         0         0         0         0
*PART
$# title
Plate
$#     pid     secid       mid     eosid      hgid      grav    adpopt      tmid
        32         1         1         0         0         0         0         0
*PART
$# title
TVoid
$#     pid     secid       mid     eosid      hgid      grav    adpopt      tmid
        38         2         2         0         0         0         0         0
*PART
$# title
LVoid
$#     pid     secid       mid     eosid      hgid      grav    adpopt      tmid
        40         2         2         0         0         0         0         0
*INITIAL_VOID_SET
$#    psid
         4
*DEFINE_CURVE
$#    lcid      sidr       sfa       sfo      offa      offo    dattyp
         1         0  1.000000  1.000000     0.000     0.000         0
$#                a1                  o1
               0.000        -100.0000000
           0.0600000        -100.0000000
           0.0600100               0.000
*SET_PART_LIST_TITLE
Rigids
$#     sid       da1       da2       da3       da4
         2     0.000     0.000     0.000     0.000
$#    pid1      pid2      pid3      pid4      pid5      pid6      pid7      pid8
         6        32         1         0         0         0         0         0
*SET_PART_LIST_TITLE
ALEs
$#     sid       da1       da2       da3       da4
         3     0.000     0.000     0.000     0.000
$#    pid1      pid2      pid3      pid4      pid5      pid6      pid7      pid8
        28        26        38        40         0         0         0         0
*SET_PART_LIST_TITLE
Voids
$#     sid       da1       da2       da3       da4
         4     0.000     0.000     0.000     0.000
$#    pid1      pid2      pid3      pid4      pid5      pid6      pid7      pid8
        38        28        40         0         0         0         0         0
*CONSTRAINED_LAGRANGE_IN_SOLID
$#   slave    master     sstyp     mstyp     nquad     ctype     direc     mcoup
         2         3         0         0         3         2         1         0
```

```
$#   start        end       pfac       fric     frcmin       norm    normtyp       damp
     0.0001.0000E+10  0.100000      0.000  0.500000          0          0          0
$#      cq       hmin       hmax      ileak      pleak    lcidpor      nvent   blockage
     0.000      0.000      0.000          0  0.010000          0          0          0
$#  iboxid    ipenchk    intforc    ialesof     lagmul     pfacmm       thkf
         0          0          0          0      0.000          0      0.000
*ELEMENT_SOLID
$#   eid      pid       n1       n2       n3       n4       n5       n6       n7       n8
      17        1        1       33        3        2       34       37       36       35
        .
        .
        .
   568556       40   596242   569048   569050   564082   596243   569051   569053   564086
*NODE
$#   nid               x               y               z      tc      rc
       1      25.0000000  1.1389044e-013      23.5000000       0       0
        .
        .
        .
        596288     -29.9999981      -4.8812861     -27.8697014       0       0
*END
```

Modified RBM setup

GeneralControlDatabase

```
$# LS-DYNA Keyword file created by LS-PrePost 4.2 (Alpha) - 13May2014(23:00)
$# Created on May-15-2014 (10:22:03)
*KEYWORD MEMORY=250000000
*TITLE
$# title
LS-DYNA keyword deck by LS-PrePost
*CONTROL_ALE
$#     dct       nadv       meth       afac       bfac       cfac       dfac       efac
         1          1          1 -1.000000      0.000      0.000      0.000      0.000
$#   start        end      aafac      vfact       prit        ebc       pref    nsidebc
     0.0001.0000E+20  1.000000 1.0000E-6          0          0      0.000          0
$#    ncpl       nbkt     imascl     checkr
         1         50          0      0.000
*CONTROL_BULK_VISCOSITY
$#      q1         q2       type      btype
  1.500000 6.0000E-2         -1          0
*CONTROL_CONTACT
$#  slsfac     rwpnal     islchk     shlthk     penopt     thkchg      orien     enmass
  0.100000  1.000000          2          0          1          1          1          0
$#  usrstr     usrfrc      nsbcs     interm      xpene      ssthk       ecdt    tiedprj
         1          0          0          0      0.000          0          0          0
$#   sfric      dfric        edc        vfc         th      th_sf     pen_sf
     0.000      0.000      0.000      0.000      0.000      0.000      0.000
$#  ignore     frceng    skiprwg     outseg    spotstp    spotdel    spothin
         1          0          0          0          0          0      0.000
$#    isym     nserod     rwgaps     rwgdth      rwksf       icov     swradf     ithoff
         0          0          1      0.000  1.000000          0      0.000          0
$#  shledg     pstiff     ithcnt     tdcnof      ftall     unused     shltrw
         0          0          0          0          0                 0.000
*CONTROL_ENERGY
$#    hgen       rwen     slnten      rylen
```

```
         2         2         2         1
*CONTROL_HOURGLASS
$#     ihq        qh
         1  0.100000
*CONTROL_MPP_DECOMPOSITION_DISTRIBUTE_ALE_ELEMENTS
*CONTROL_SHELL
$#  wrpang     esort     irnxx    istupd    theory       bwc     miter      proj
 70.000000         1        -1         1         2         2         1         0
$# rotascl    intgrd    lamsht    cstyp6    tshell
  1.000000         0         0         1         0         0         0         0
$# psstupd   sidt4tu     cntco    itsflg    irquad
         0         0         0         0         2
*CONTROL_TERMINATION
$#  endtim    endcyc     dtmin    endeng    endmas
 5.0000E-4         0     0.000     0.000     0.000
*DATABASE_BINARY_D3PLOT
$#      dt      lcdt      beam     npltc    psetid
 1.0000E-5         0         2         0         0
$#   ioopt
         0
*DATABASE_EXTENT_BINARY
$#   neiph     neips    maxint    strflg    sigflg    epsflg    rltflg    engflg
         0         0         3         1         1         1         1         1
$#  cmpflg    ieverp    beamip     dcomp      shge     stssz    n3thdt   ialemat
         0         0         0         1         1         1         2         1
$# nintsld   pkp_sen      sclp     hydro     msscl     therm    intout    nodout
         0         0     0.000         0         0         0STRESS
$#    dtdt    resplt
         0         0
*HOURGLASS
$#    hgid       ihq        qm       ibq        q1        q2    qb/vdc        qw
         1         1 5.0000E-3         0  1.500000 6.0000E-2  0.100000  0.100000
*DAMPING_GLOBAL
$#    lcid    valdmp       stx       sty       stz       srx       sry       srz
         0  0.100000     0.000     0.000     0.000     0.000     0.000     0.000
*END
```

RatHead_Geometry

```
$# LS-DYNA Keyword file created by LS-PrePost 4.1 - 09May2014(08:00)
$# Created on Jul-16-2014 (10:03:57)
*KEYWORD
*TITLE
$# title
JARI_Chalmers_RatHeadFEmodel_v1_mod
*PART
$# title
OLF_VOID
$#     pid     secid       mid     eosid      hgid      grav    adpopt      tmid
        26        11        11         0         0         0         0         0
*PART
$# title
CORTEX_VOID
$#     pid     secid       mid     eosid      hgid      grav    adpopt      tmid
        27        11        11         0         0         0         0         0
*PART
```

```
$# title
THA_VOID
$#     pid     secid       mid     eosid      hgid      grav    adpopt      tmid
        28        11        11         0         0         0         0         0
*PART
$# title
BRA_VOID
$#     pid     secid       mid     eosid      hgid      grav    adpopt      tmid
        30        11        11         0         0         0         0         0
*PART
$# title
CER_VOID
$#     pid     secid       mid     eosid      hgid      grav    adpopt      tmid
        31        11        11         0         0         0         0         0
*PART
$# title
SPINE_VOID
$#     pid     secid       mid     eosid      hgid      grav    adpopt      tmid
        37        11        11         0         0         0         0         0
*PART
$# title
BOLT
$#     pid     secid       mid     eosid      hgid      grav    adpopt      tmid
        39        10        10         0         0         0         0         0
*ELEMENT_SOLID
$#   eid     pid      n1      n2      n3      n4      n5      n6      n7      n8
   16397       2    2073   14064   17724   66122    7722    7437    7269   10252
      .
      .
      .
  143537      10  122973  122985  123304  123304       0       0       0       0
*NODE
$#   nid               x               y               z      tc      rc
     127       12.183913       25.934261      100.600502       0       0
      .
      .
      .
     607       15.643964       25.944407      101.590897       0       0
*BOUNDARY_SPC_NODE
$#     nid       cid      dofx      dofy      dofz     dofrx     dofry     dofrz
     95679         0         1         1         1         1         1         1
      .
      .
      .
*BOUNDARY_SPC_SET_BIRTH_DEATH
$#    nsid       cid      dofx      dofy      dofz     dofrx     dofry     dofrz
         1         0         1         0         1         1         1         1
$#   birth     death
     0.000     0.000
*SET_NODE_LIST_TITLE
NODESET(SPC) 1
$#     sid       da1       da2       da3       da4    solver
         1     0.000     0.000     0.000     0.000MECH
$#    nid1      nid2      nid3      nid4      nid5      nid6      nid7      nid8
    304237    304238    304239    304240    304241    304242    304243    304244
      .
```

```
      .
      .
    305829    305830    305831         0         0         0         0         0
*END
```

RatHead_NoGeometry

```
$# LS-DYNA Keyword file created by LS-PrePost 4.1 - 09May2014(08:00)
$# Created on Jul-16-2014 (10:08:57)
*KEYWORD MEMORY=250000000
*TITLE
$# title
LS-DYNA keyword deck by LS-Prepost
    .
    .
    .
*SECTION_SOLID_TITLE
THAL
$#   secid    elform       aet
         7        11         0
         .
         .
         .
*ALE_REFERENCE_SYSTEM_GROUP
$#     sid     stype    prtype      prid    bctran     bcexp     bcrot    icoord
         5         0         4         0         0         0         0         0
$#      xc        yc        zc    explim      efac    unused    frcpad   iexpnd
     0.000     0.000     0.000     0.000     0.000             0.100000         0
*ALE_MULTI-MATERIAL_GROUP_SET
$#    psid
         6
         8
         9
*ALE_MULTI-MATERIAL_GROUP_PART
         2
         3
         4
*ALE_MULTI-MATERIAL_GROUP_SET
        10
*BOUNDARY_PRESCRIBED_MOTION_RIGID_ID
$#      id                                                               heading
         0BoltMovement
$#     pid       dof       vad      lcid        sf       vid     death     birth
        39         2         0        10  1.000000         01.0000E+28     0.000
*CONSTRAINED_LAGRANGE_IN_SOLID_TITLE
$#  coupid                                                                 title
         0BOLT vs ALEs
$#   slave    master     sstyp     mstyp     nquad     ctype     direc     mcoup
        39         5         1         0         2         4         2         0
$#   start       end      pfac      fric    frcmin      norm   normtyp      damp
     0.0001.0000E+10  0.100000     0.000  0.500000         0         0     0.000
$#      cq      hmin      hmax    ileak     pleak   lcidpor     nvent  blockage
     0.000     0.000     0.000         0 1.0000E-2         0         0         0
$#  iboxid   ipenchk   intforc   ialesof    lagmul    pfacmm      thkf
         0         0         0         0     0.000         0     0.000
*CONSTRAINED_LAGRANGE_IN_SOLID_TITLE
```

```
$#  coupid                                                                 title
         OSKULL vs TISSUE
$#   slave    master     sstyp     mstyp     nquad     ctype     direc     mcoup
         4         7         0         0         2         4         2         0
$#   start       end      pfac      fric    frcmin      norm   normtyp      damp
     0.0001.0000E+10  0.100000     0.000  0.500000         0         0     0.000
$#      cq      hmin      hmax     ileak     pleak   lcidpor     nvent  blockage
     0.000     0.000     0.000         0 1.0000E-2         0         0         0
            .
            .
            .
*DEFINE_CURVE_TITLE
BOLT_CURVE
$#    lcid      sidr       sfa       sfo      offa      offo    dattyp
        10         0     0.000     0.000     0.000     0.000         0
$#                a1                  o1
               0.000          100.000000
       6.700000e-005          100.000000
       6.700100e-005               0.000
       1.000000e-004               0.000
       .
       .
       .
*MAT_RIGID_TITLE
BOLT
$#     mid        ro         e        pr         n    couple         m     alias
        10 2700.00007.0000E+10  0.350000     0.000     0.000     0.000
$#     cmo      con1      con2
     0.000        0.        0.
$# lco or a1      a2        a3        v1        v2        v3
     0.000     0.000     0.000     0.000     0.000     0.000
*MAT_VACUUM_TITLE
VACUUM
$#     mid       den
        11 1.0000E-3
*SECTION_SOLID_TITLE
BOLT
$#   secid    elform       aet
        10         1         0
*SECTION_SOLID_ALE_TITLE
VOIDS
$#   secid    elform       aet
        11        11         1
$#    afac      bfac      cfac      dfac     start       end     aafac
     0.000     0.000     0.000     0.000     0.000     0.000     0.000
*SET_PART_LIST_TITLE
INTERIOR
$#     sid       da1       da2       da3       da4    solver
         3  1.000000  0.2000001.0000E+10  1.000000MECH
$#    pid1      pid2      pid3      pid4      pid5      pid6      pid7      pid8
         1         2         3         4         5         6         7         8
*SET_PART_LIST_TITLE
Skull and C2
$#     sid       da1       da2       da3       da4    solver
         4  1.000000  0.2000001.0000E+10  1.000000MECH
$#    pid1      pid2      pid3      pid4      pid5      pid6      pid7      pid8
```

```
        10        22         0         0         0         0         0         0
*SET_PART_LIST_TITLE
ALEs
$#     sid       da1       da2       da3       da4    solver
         5     0.000     0.000     0.000     0.000MECH
$#    pid1      pid2      pid3      pid4      pid5      pid6      pid7      pid8
         1         2         3         4         5         6         7         8
         9        26        27        28        30        31        37         0
*SET_PART_LIST_TITLE
Voids
$#     sid       da1       da2       da3       da4    solver
         6     0.000     0.000     0.000     0.000MECH
$#    pid1      pid2      pid3      pid4      pid5      pid6      pid7      pid8
        26        27        28        30        31        37         0         0
*SET_PART_LIST_TITLE
TissueALEs
$#     sid       da1       da2       da3       da4    solver
         7     0.000     0.000     0.000     0.000MECH
$#    pid1      pid2      pid3      pid4      pid5      pid6      pid7      pid8
         1         2         3         4         5         6         7         8
         9         0         0         0         0         0         0         0
*SET_PART_LIST_TITLE
MMALE1
$#     sid       da1       da2       da3       da4    solver
         8     0.000     0.000     0.000     0.000MECH
$#    pid1      pid2      pid3      pid4      pid5      pid6      pid7      pid8
         6         9         0         0         0         0         0         0
*SET_PART_LIST_TITLE
MMALE2
$#     sid       da1       da2       da3       da4    solver
         9     0.000     0.000     0.000     0.000MECH
$#    pid1      pid2      pid3      pid4      pid5      pid6      pid7      pid8
         7         8         0         0         0         0         0         0
*SET_PART_LIST_TITLE
MMALE3
$#     sid       da1       da2       da3       da4    solver
        10  1.000000  0.2000001.0000E+10  1.000000MECH
$#    pid1      pid2      pid3      pid4      pid5      pid6      pid7      pid8
         1         5         0         0         0         0         0         0
$
$Unrecognized cards
$
$         0         0
*END
```

RBM variable variation setup

RatHead_NoGeometry_angled10degrees

```
$# LS-DYNA Keyword file created by LS-PrePost 4.1 - 09May2014(08:00)
$# Created on Jul-28-2014 (14:41:55)
*KEYWORD MEMORY=250000000
*TITLE
$# title
LS-DYNA keyword deck by LS-Prepost
    .
    .
```

```
    .
    *BOUNDARY_PRESCRIBED_MOTION_RIGID_ID
$#        id                                                               heading
           0BoltMovementY
$#       pid       dof       vad      lcid        sf       vid     death     birth
          39         2         0        10  1.000000          01.0000E+28     0.000
$#        id                                                               heading
           0BoltMovementZ
$#       pid       dof       vad      lcid        sf       vid     death     birth
          39         3         0        11  1.000000          01.0000E+28     0.000
$#        id                                                               heading
           0BoltLockedX
$#       pid       dof       vad      lcid        sf       vid     death     birth
          39         1         2        20  1.000000          01.0000E+28     0.000
$#        id                                                               heading
           0BoltLockedY
$#       pid       dof       vad      lcid        sf       vid     death     birth
          39         2         2        20  1.000000          01.0000E+28 6.7100E-5
$#        id                                                               heading
           0BoltLockedZ
$#       pid       dof       vad      lcid        sf       vid     death     birth
          39         3         2        20  1.000000          01.0000E+28 6.7100E-5
$#        id                                                               heading
           0BoltLockedRX
$#       pid       dof       vad      lcid        sf       vid     death     birth
          39         5         2        20  1.000000          01.0000E+28 6.7100E-5
$#        id                                                               heading
           0BoltLockedRZ
$#       pid       dof       vad      lcid        sf       vid     death     birth
          39         7         2        20  1.000000          01.0000E+28 6.7100E-5
$#        id                                                               heading
           0BoltLockedRY
$#       pid       dof       vad      lcid        sf       vid     death     birth
          39         6         2        20  1.000000          01.0000E+28 6.7100E-5
            .
            .
            .
BOLT_CURVE_Y
$#      lcid      sidr       sfa       sfo      offa      offo    dattyp
          10         0     0.000     0.000     0.000     0.000         0
$#                  a1                  o1
                 0.000           98.480797
          6.700000e-005           98.480797
          6.700100e-005               0.000
*DEFINE_CURVE_TITLE
BOLT_CURVE_Z
$#      lcid      sidr       sfa       sfo      offa      offo    dattyp
          11         0     0.000     0.000     0.000     0.000         0
$#                  a1                  o1
                 0.000          -17.364799
          6.700000e-005          -17.364799
          6.700100e-005               0.000
        .
        .
        .
*END
```

RatHead_NoGeometry_angled20degrees

```
$# LS-DYNA Keyword file created by LS-PrePost 4.1 - 09May2014(08:00)
$# Created on Jul-31-2014 (10:57:47)
*KEYWORD MEMORY=250000000
*TITLE
$# title
LS-DYNA keyword deck by LS-Prepost
     .
     .
     .
*BOUNDARY_PRESCRIBED_MOTION_RIGID_ID
$#      id                                                           heading
         0BoltMovementY
$#     pid       dof       vad      lcid        sf       vid     death     birth
        39         2         0        10  1.000000         01.0000E+28     0.000
$#      id                                                           heading
         0BoltMovementZ
$#     pid       dof       vad      lcid        sf       vid     death     birth
        39         3         0        11  1.000000         01.0000E+28     0.000
$#      id                                                           heading
         0BoltLockedX
$#     pid       dof       vad      lcid        sf       vid     death     birth
        39         1         2        20  1.000000         01.0000E+28     0.000
$#      id                                                           heading
         0BoltLockedY
$#     pid       dof       vad      lcid        sf       vid     death     birth
        39         2         2        20  1.000000         01.0000E+28 6.7100E-5
$#      id                                                           heading
         0BoltLockedZ
$#     pid       dof       vad      lcid        sf       vid     death     birth
        39         3         2        20  1.000000         01.0000E+28 6.7100E-5
$#      id                                                           heading
         0BoltLockedRX
$#     pid       dof       vad      lcid        sf       vid     death     birth
        39         5         2        20  1.000000         01.0000E+28 6.7100E-5
$#      id                                                           heading
         0BoltLockedRZ
$#     pid       dof       vad      lcid        sf       vid     death     birth
        39         7         2        20  1.000000         01.0000E+28 6.7100E-5
$#      id                                                           heading
         0BoltLockedRY
$#     pid       dof       vad      lcid        sf       vid     death     birth
        39         6         2        20  1.000000         01.0000E+28 6.7100E-5
         .
         .
         .
*DEFINE_CURVE_TITLE
BOLT_CURVE_Y
$#    lcid      sidr       sfa       sfo      offa      offo    dattyp
        10         0     0.000     0.000     0.000     0.000         0
$#                a1                  o1
               0.000           93.969299
       6.700000e-005           93.969299
       6.700100e-005               0.000
*DEFINE_CURVE_TITLE
```

```
BOLT_CURVE_Z
$#    lcid      sidr       sfa       sfo      offa      offo    dattyp
        11         0     0.000     0.000     0.000     0.000         0
$#                a1                  o1
               0.000          -34.202000
       6.700000e-005          -34.202000
       6.700100e-005               0.000
       .
       .
       .
*END
```